Deeply Virtual Compton Scattering on Longitudinally Polarized Protons at CLAS

Erin Seder

April 25, 2014

Nucleon Structure

Through Deep Exclusive Reactions

- Measurements of cross sections and asymmetries in Deep Exclusive Reactions:

Deeply Virtual Compton Scattering

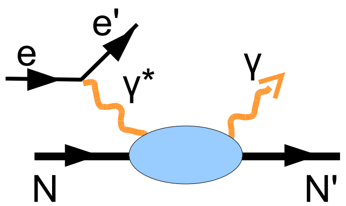

Deeply Virtual Meson Production

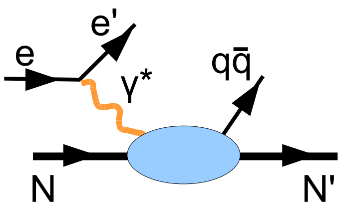

Access **Generalized Parton Distributions (GPDs)**
Relate transverse position of partons to their longitudinal momentum

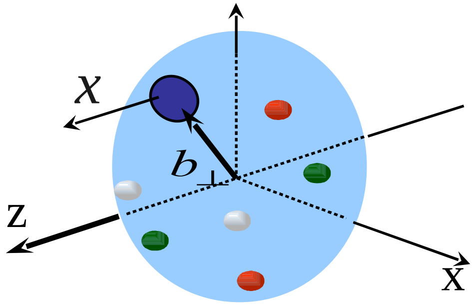

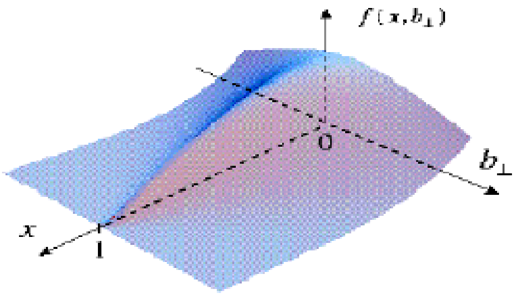

Deeply Virtual Compton Scattering and Generalized Parton Distributions

$Q^2 = -(p_e - p_{e'})^2$ **Large, with** $Q^2 \gg t = (p_p - p_{p'})^2$

and fixed $x_B = \dfrac{Q^2}{2 M_p \nu}$, $(\nu = E_e - E_{e'})$

factorization:

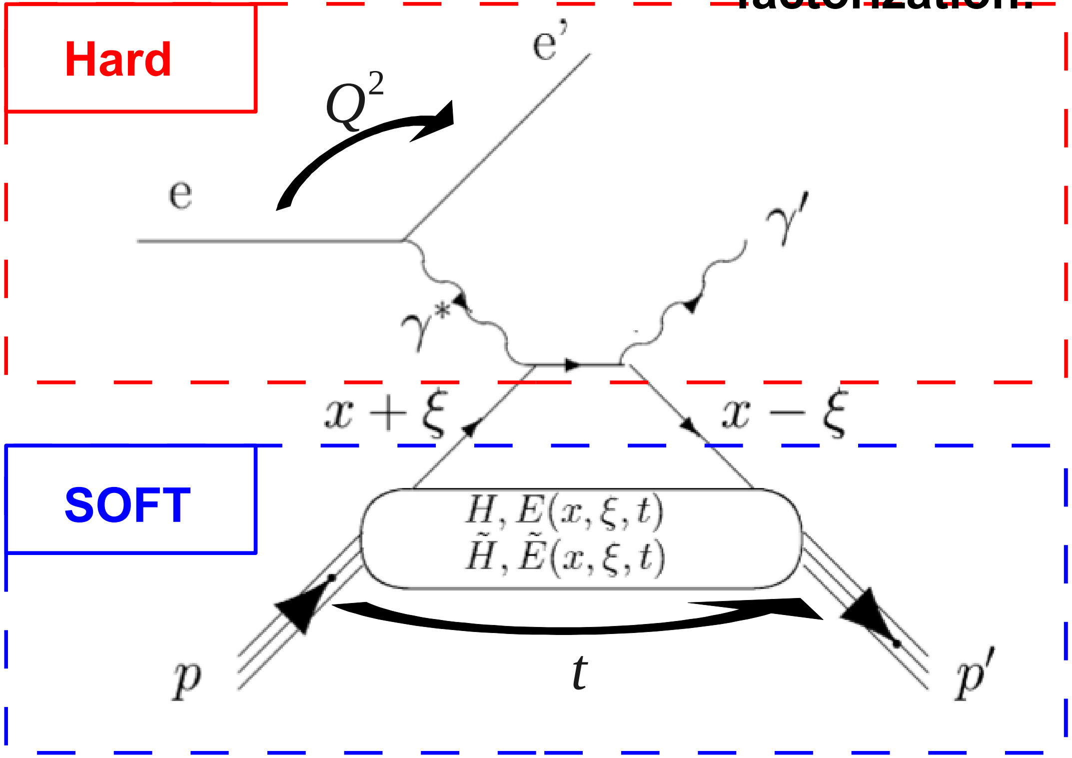

soft part described by 4 GPDs at LO

Generalized Parton Distributions (GPDs)

$$\boldsymbol{H}(x,\xi,t), \boldsymbol{E}(x,\xi,t)$$
$$\tilde{\boldsymbol{H}}(x,\xi,t), \tilde{\boldsymbol{E}}(x,\xi,t)$$

x : longitudinal quark momentum fraction (not experimentally accessible)

2ξ : longitudinal momentum transfer. In the Bjorken limit:

$$\xi \simeq \frac{x_B}{2 - x_B}$$

t : total squared momentum transfer to the nucleon

$$t = (p_p - p_{p'})^2$$

Generalized Parton Distributions

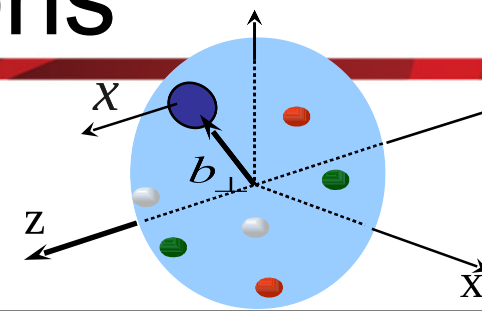

$$\boldsymbol{H}(x,\xi,t),\boldsymbol{E}(x,\xi,t)$$
$$\tilde{\boldsymbol{H}}(x,\xi,t),\tilde{\boldsymbol{E}}(x,\xi,t)$$

Form Factors (FFs)

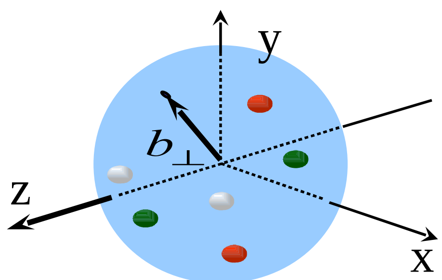

$$\int_{-1}^{+1} dx\, \boldsymbol{H}^q(x,\xi,t) = F_1^q(t)$$ Dirac

$$\int_{-1}^{+1} dx\, \boldsymbol{E}^q(x,\xi,t) = F_2^q(t)$$ Pauli

$$\int_{-1}^{+1} dx\, \tilde{\boldsymbol{H}}^q(x,\xi,t) = G_A^q(t)$$ axial

$$\int_{-1}^{+1} dx\, \tilde{\boldsymbol{E}}^q(x,\xi,t) = G_P^q(t)$$ pseudo-scalar

Parton Distribution Functions (PDFs)

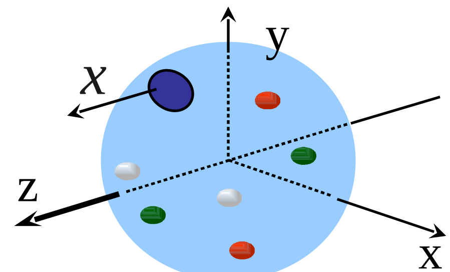

$$\boldsymbol{H}^q(x,0,0) = \begin{cases} q(x), & x>0 \\ -\bar{q}(-x), & x<0 \end{cases}$$ unpolarized quark distributions

$$\tilde{\boldsymbol{H}}^q(x,0,0) = \begin{cases} \Delta q(x), & x>0 \\ \Delta \bar{q}(-x), & x<0 \end{cases}$$ polarized quark distributions

New information such as:

Angular Momentum Sum Rule

$$J_q = \frac{1}{2}\int_{-1}^{+1} dx\; x\; [\boldsymbol{H}^q(x,\xi,0)+\boldsymbol{E}^q(x,\xi,0)]$$

X. Ji, Phy.Rev.Lett.78,610(1997)

Accessing GPDs through DVCS

$$\frac{d\sigma}{dx_B\, dQ^2\, d|t|\, d\phi} = \frac{x_B e^6 |\tau|^2}{32(2\pi)^2 \sqrt{Q^2 + (2x_B M_p)^2}}$$

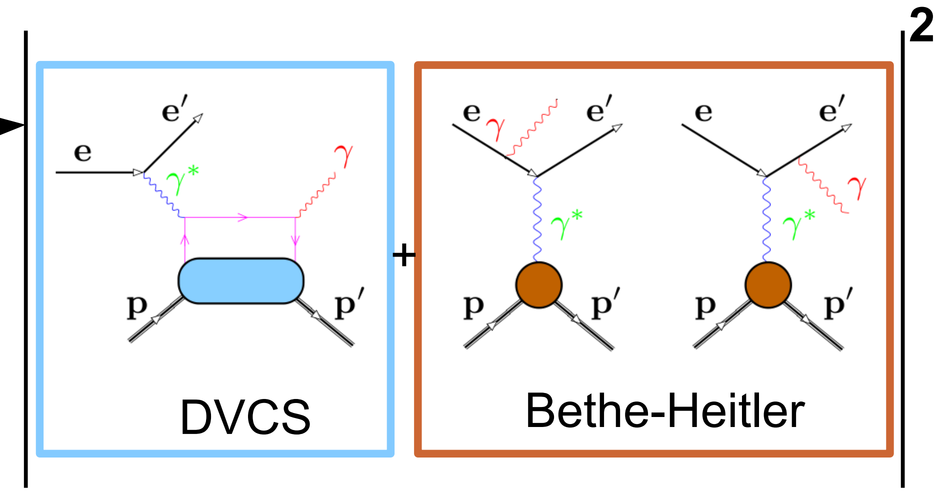

$$|\tau|^2 = |\tau_{BH}|^2 + |\tau_{DVCS}|^2 + \{\tau_{DVCS}\tau^*_{BH} + \tau^*_{DVCS}\tau_{BH}\}$$

τ_{BH} ➡ nucleon form factors F_1 and F_2

τ_{DVCS} ➡ $\displaystyle\int_{-1}^{+1} \frac{H(x,\xi,t)}{x \pm \xi \mp i\epsilon} dx + \dots$

$I = \{\tau_{DVCS}\tau^*_{BH} + \tau^*_{DVCS}\tau_{BH}\}$ ➡ linear combinations of **GPDs**

Accessing GPDs through DVCS

$$\frac{d\sigma}{dx_B\, dQ^2\, d|t|\, d\phi} = \frac{x_B e^6 |\tau|^2}{32(2\pi)^2 \sqrt{Q^2 + (2x_B M_p)^2}}$$

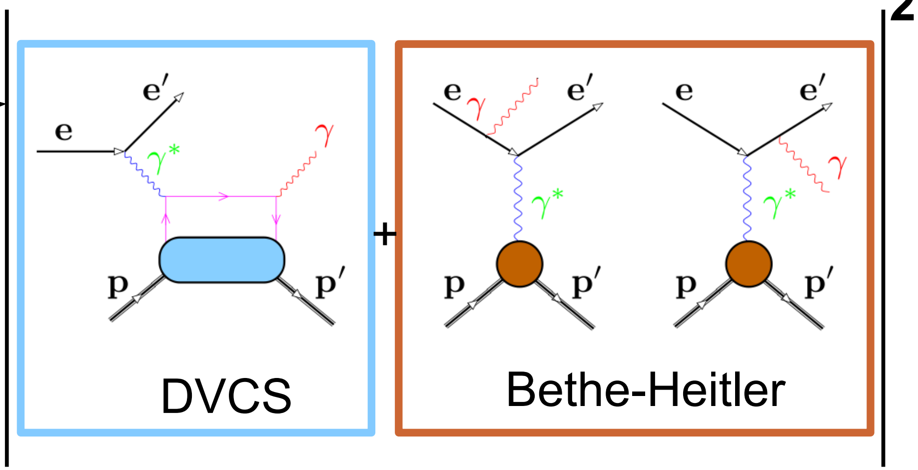

I can isolated via spin observables such as asymmetries:

$$A = \frac{\sigma^{\uparrow} - \sigma^{\downarrow}}{\sigma^{\uparrow} + \sigma^{\downarrow}} \propto \frac{I}{|\tau_{BH}|^2 + |\tau_{DVCS}|^2 + I}$$

τ_{BH} ➡ nucleon form factors F_1 and F_2

τ_{DVCS} ➡ $\displaystyle\int_{-1}^{+1} \frac{\boldsymbol{H}(x,\xi,t)}{x \pm \xi \mp i\epsilon} dx + \dots$

$I = \{\tau_{DVCS}\tau_{BH}^{*} + \tau_{DVCS}^{*}\tau_{BH}\}$ ➡ linear combinations of **GPDs**

Accessing GPDs through DVCS

$$T^{\mathrm{DVCS}} \sim \int_{-1}^{+1} \frac{\boldsymbol{H}(x,\xi,t)}{x \pm \xi \mp i\epsilon} dx + \ldots \Longrightarrow \overbrace{P\int_{-1}^{+1} \frac{\boldsymbol{H}(x,\xi,t)}{x \pm \xi} dx}^{\Re e\,\mathcal{H}} - \overbrace{i\pi \boldsymbol{H}(\pm\xi,\xi,t)}^{\Im m\,\mathcal{H}}$$

$$A = \frac{\Delta\sigma}{\sigma}$$

Polarized electron beam, unpolarized proton target (BSA):

$$\Delta\sigma_{LU} \sim \sin(\phi)\,\Im m\{F_1 \underline{\mathcal{H}} + \frac{x_B}{2-x_B}(F_1 + F_2)\underline{\tilde{\mathcal{H}}} + \frac{t}{4M^2} F_2 \underline{\mathcal{E}} + \ldots\} d\phi \Rightarrow \Im m\{\mathcal{H}_p, \tilde{\mathcal{H}}_p, \mathcal{E}_p\}$$

Unpolarized electron beam, longitudinally polarized proton target (TSA) :

$$\Delta\sigma_{\mathrm{UL}} \sim \sin(\phi)\,\Im m\{F_1 \underline{\tilde{\mathcal{H}}} + \frac{x_B}{2-x_B}(F_1 + F_2)(\underline{\mathcal{H}} + \frac{x_B}{2}\underline{\mathcal{E}}) + \ldots\} d\phi \Rightarrow \Im m\{\mathcal{H}_p, \tilde{\mathcal{H}}_p\}$$

Polarized electron beam,longitudinally polarized proton target (DSA):

$$\Delta\sigma_{\mathrm{LL}} \sim (A + B\cos(\phi))\,\Re e\{F_1 \underline{\tilde{\mathcal{H}}} + \frac{x_B}{2-x_B}(F_1 + F_2)(\underline{\mathcal{H}} + \frac{x_B}{2}\underline{\mathcal{E}}) + \ldots\} d\phi \Rightarrow \Re e\{\mathcal{H}_p, \tilde{\mathcal{H}}_p\}$$

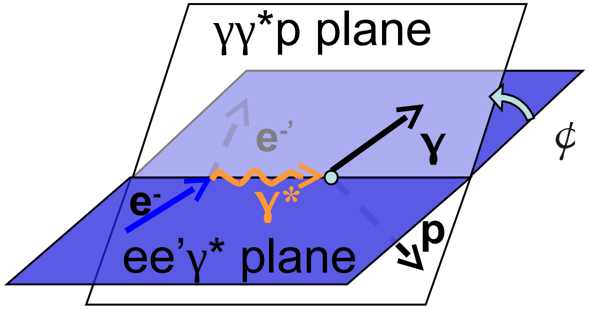

$$\xi = \frac{x_B}{2-x_B}, \quad t = (p_n - p_{n'})^2$$

Jefferson Lab & CLAS @ 6GeV

Continuous
Electron
Beam
Accelerator
Facility

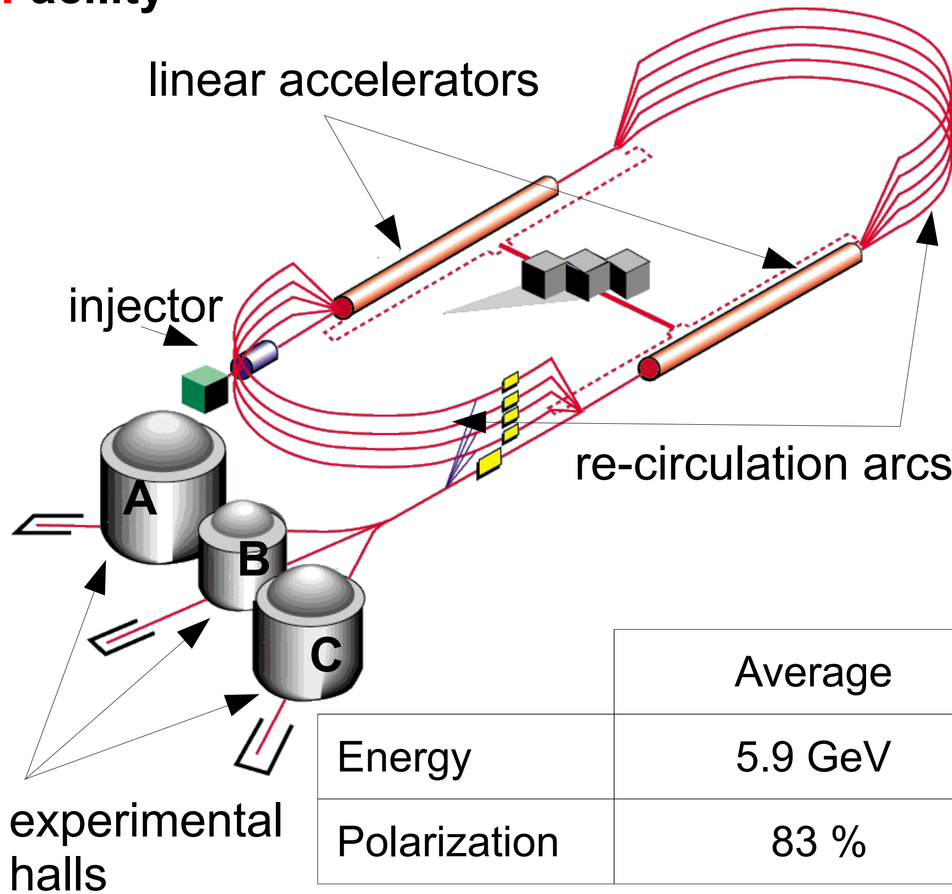

	Average
Energy	5.9 GeV
Polarization	83 %

CEBAF
Large
Acceptance
Spectrometer

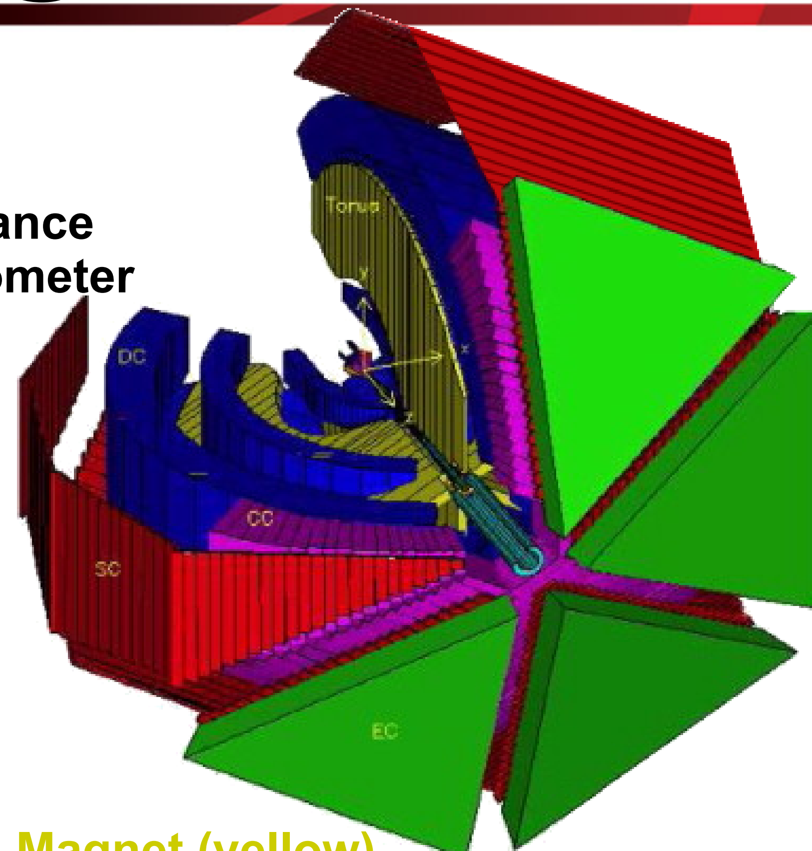

Toroidal Magnet (yellow)

-> bends charged particles towards(away) from the beamline

->splits the detector into 6 sectors in φ

Each sector:

3 segments of Drift Chambers (blue)
Cerenkov Detectors (pink)
Scintillation Counters (red)
Electromagnetic Calorimeters (green)

Previous CLAS DVCS Measurements

Non-dedicated experiment:

Beam-spin asymmetry

S. Stepanyan et al., PRL 87 (2001).

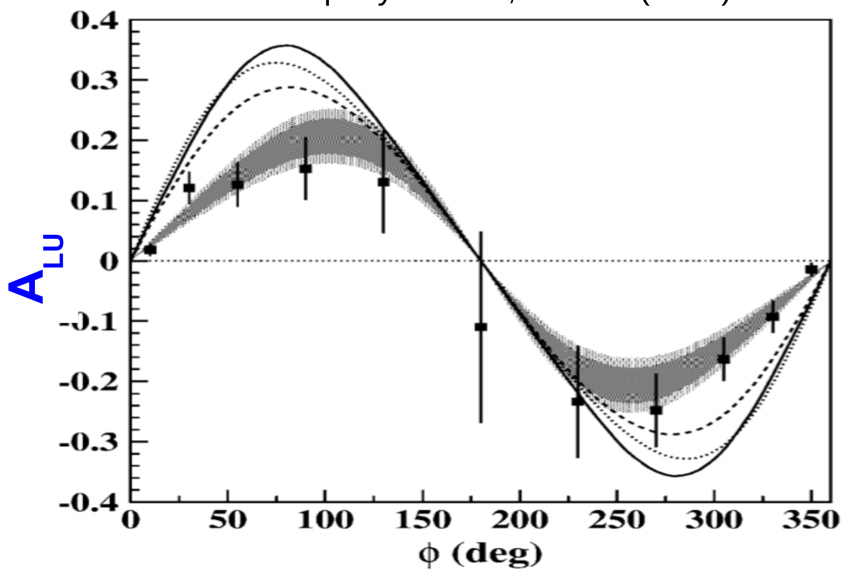

Target-spin asymmetry

S. Chen et al., PRL 97(2006).

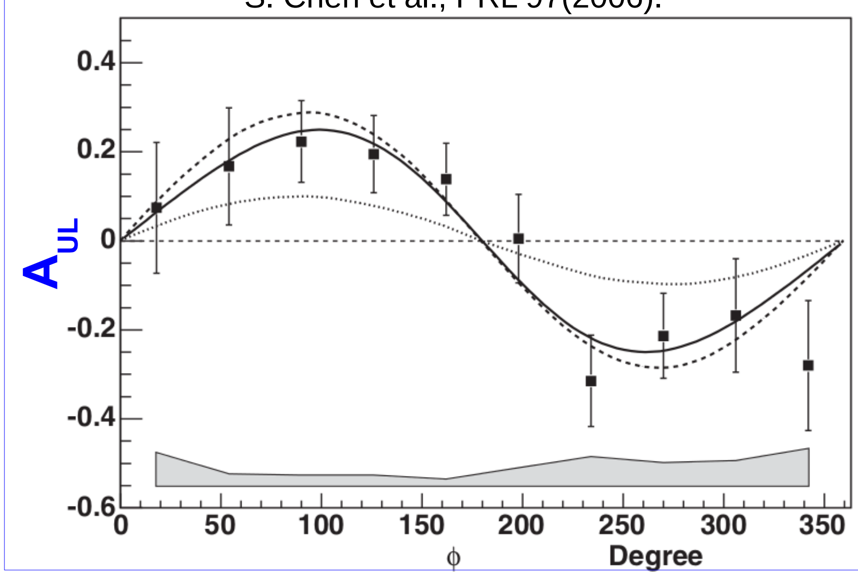

Dedicated experiment:

F.X. Girod et al., PRL 100 (2008).

E1-DVCS PR-01-113

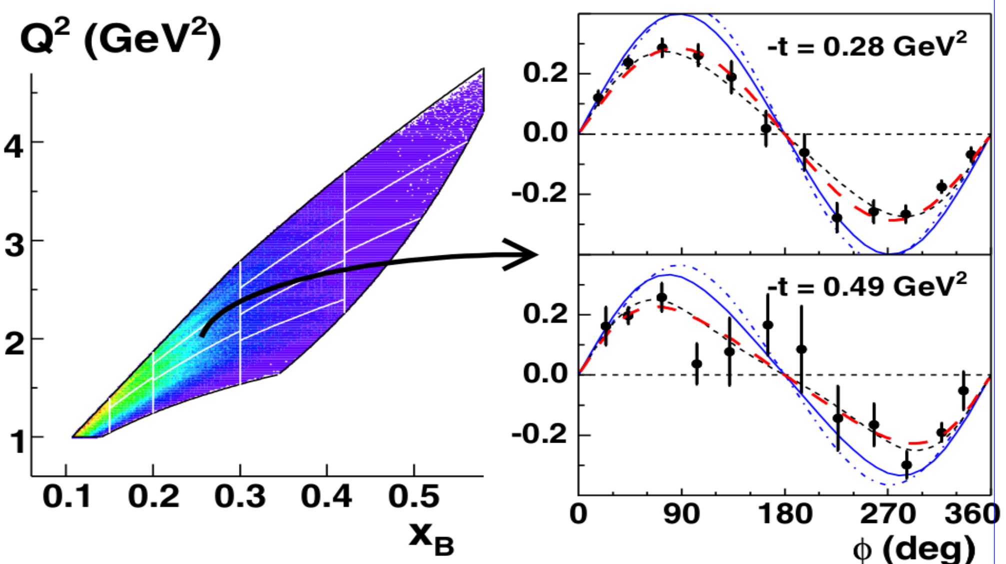

EG1-DVCS PR-05-114

This work:

~62 times more statistics than the previous CLAS measurement. This allowed for full 4-dimensional binning in kinematics:

$$Q^2,\ x_B,\ -t \text{ and } \phi$$

EG1-DVCS Experiment

IC: Inner Calorimeter

increased coverage of low angle photons:

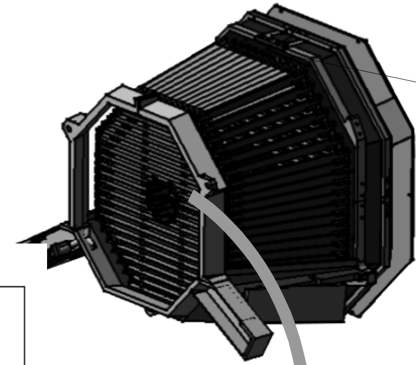

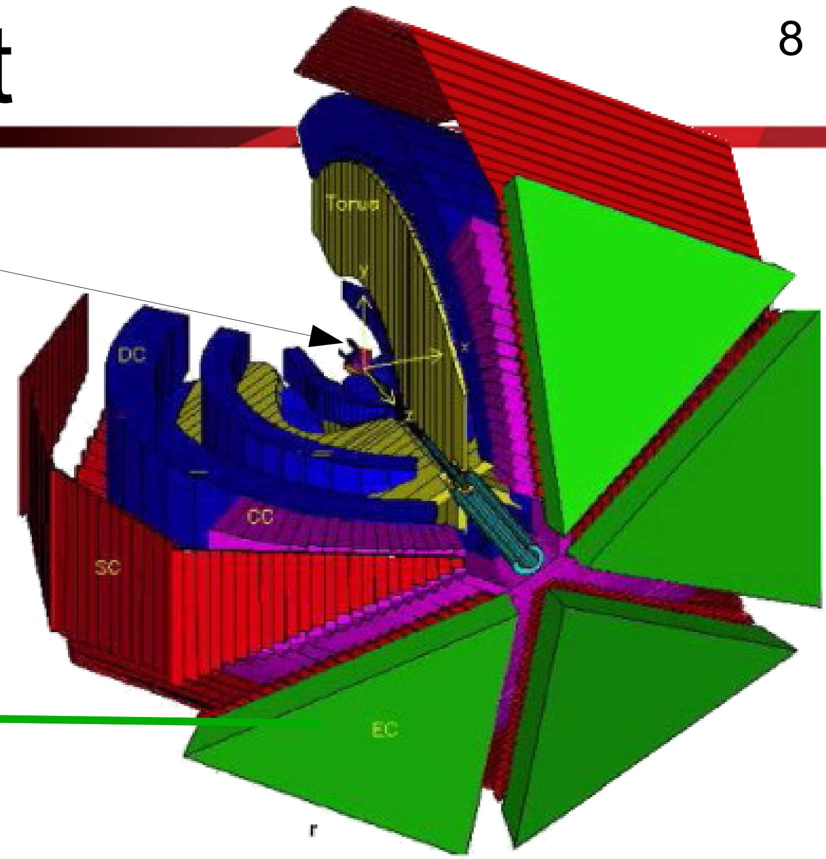

Photon coverage CLAS + IC

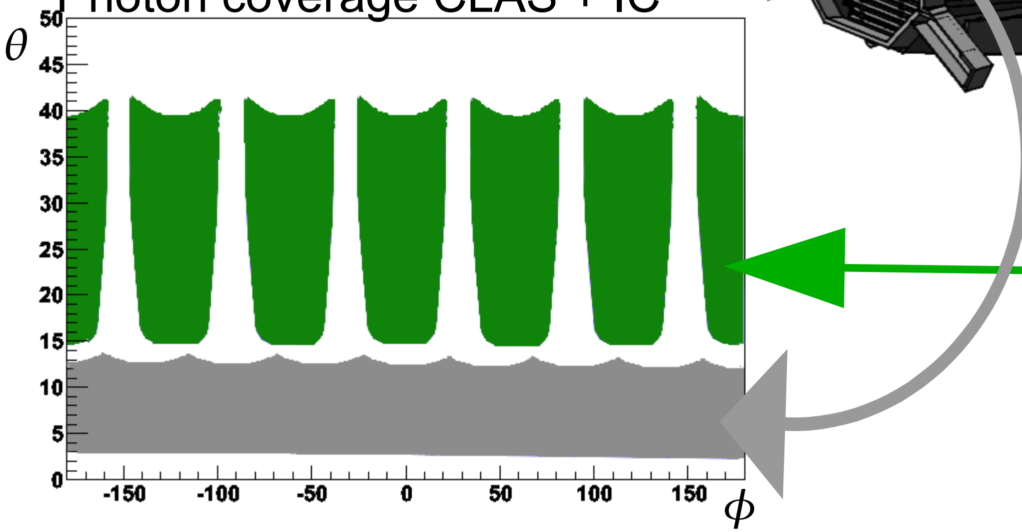

Polarized Target

Solid beads of $^{14}NH_3$

Continuously polarized via DNP

Average proton polarization ~79%

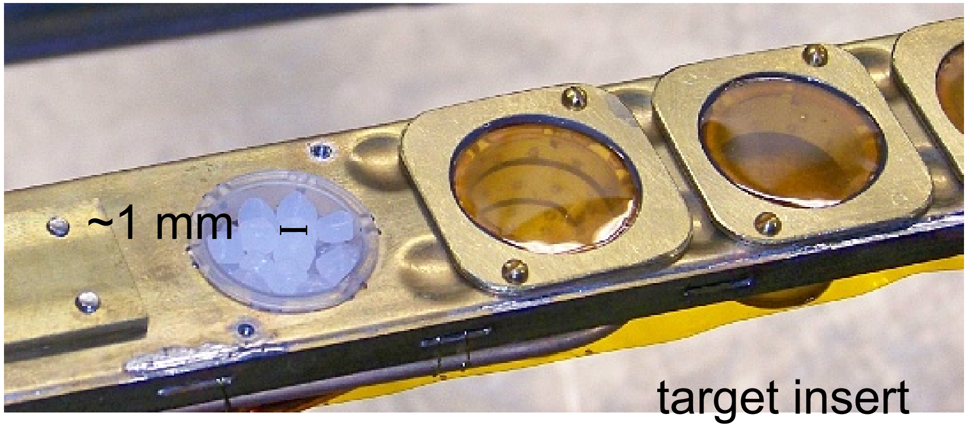

Event Selection (particle ID)

Electron:

Negative Charge
Momentum > 0.8 GeV
| Vertex – Nominal | <= 3 cm
| timing difference CC – SC | <= 2ns
Energy deposited inner EC > 0.06 GeV
EC Fiducial cut
IC Shadow Cut

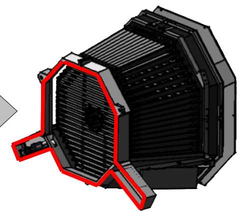

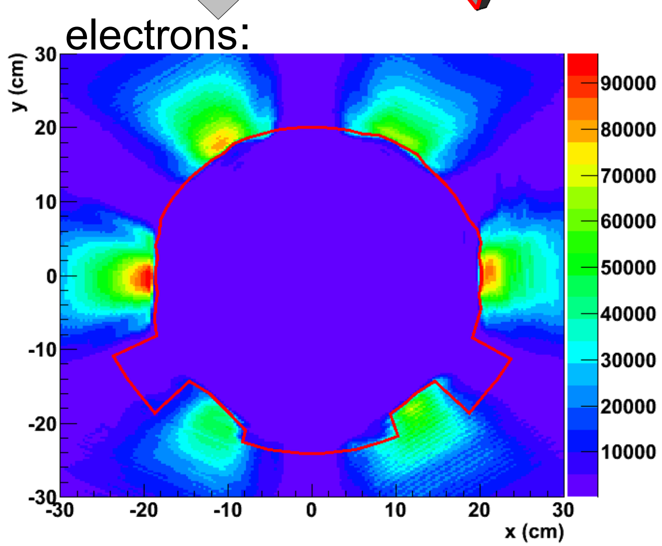

Proton:

Positive Charge
| Vertex – Nominal | <= 4 cm
Momentum dependent β Cut
IC Shadow Cut

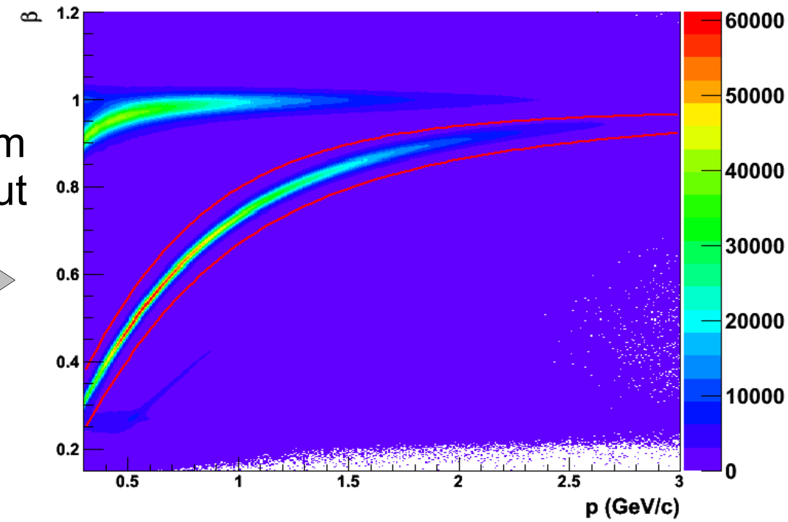

IC Photon:

IC Fiducial Cut

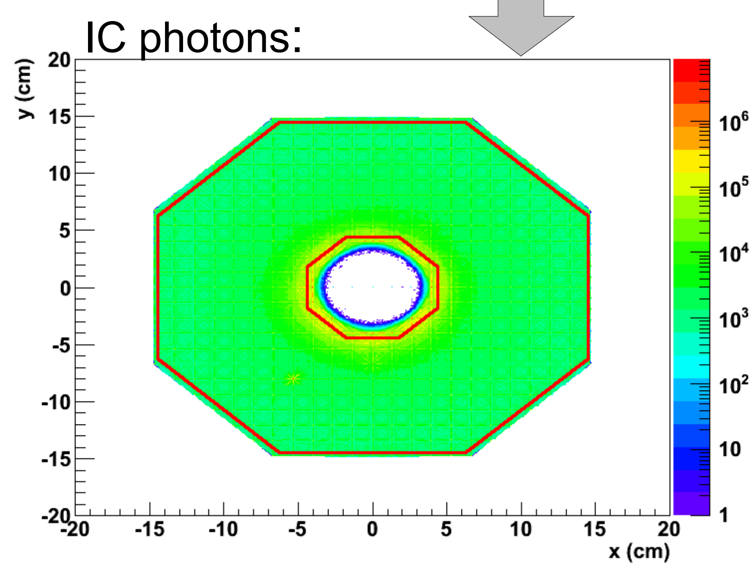

EC Photon:

Neutral Charge
Energy > 0.25 GeV
β > 0.92
EC Fiducial cut
IC Shadow Cut

Event Selection ($e\,p \rightarrow e\,p\,\gamma$)

"Deep Inelastic Scattering" regime:

$Q^2 > 1\ (GeV/c)^2$ Momentum transfer squared of the electron

$W > 2\ GeV/c^2$ Mass of the system recoiling against the scattered electron

$E_\gamma > 1\ GeV\ \ (Q^2 \gg -t)$ detected photon energy

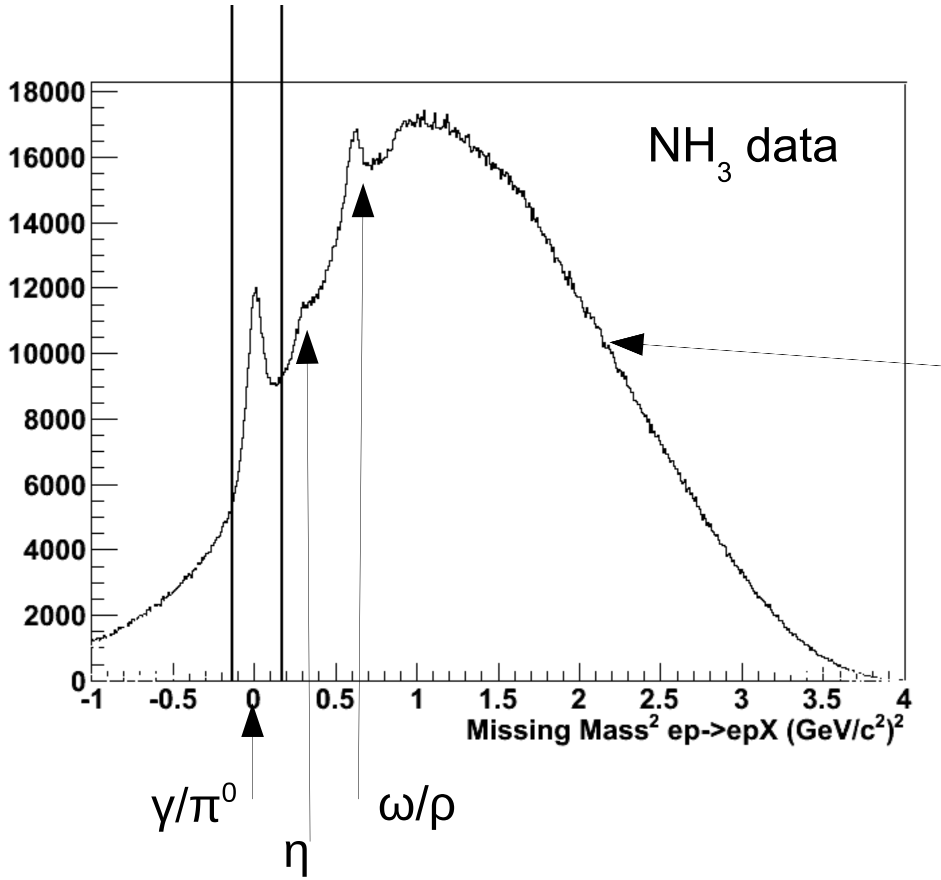

Missing mass squared of ep->epX of events with epγ detected

Large nuclear background estimate with carbon data

Event Selection ($e\,p \rightarrow e\,p\,\gamma$)

θ(γ-X) – angle between detected and expected photon

ΔΦ – difference in calculated Φ angle
1) using e, e', p
2) using e, e', γ

pPerp – missing (x,y) momentum of ep->epγ

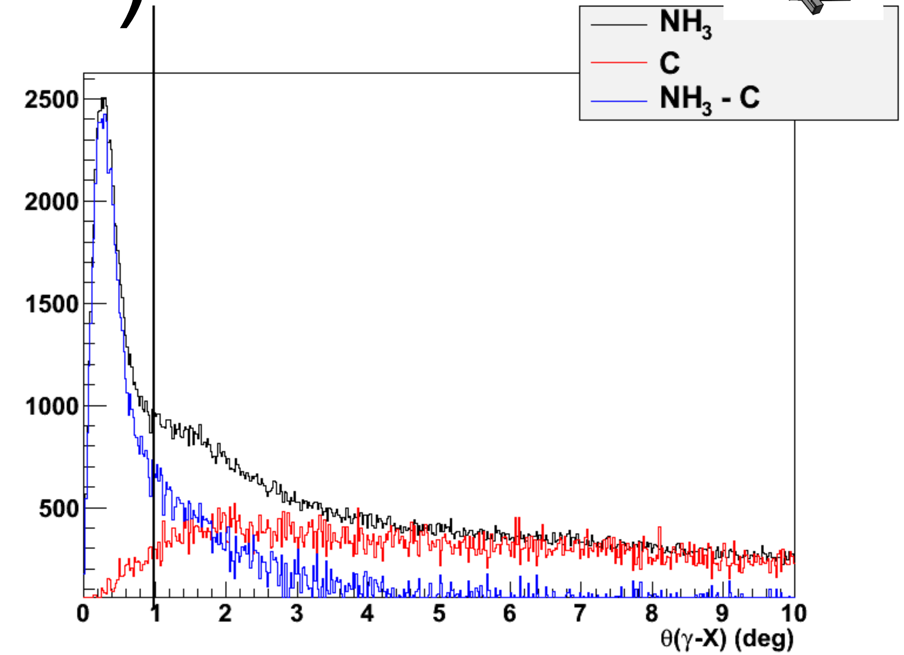

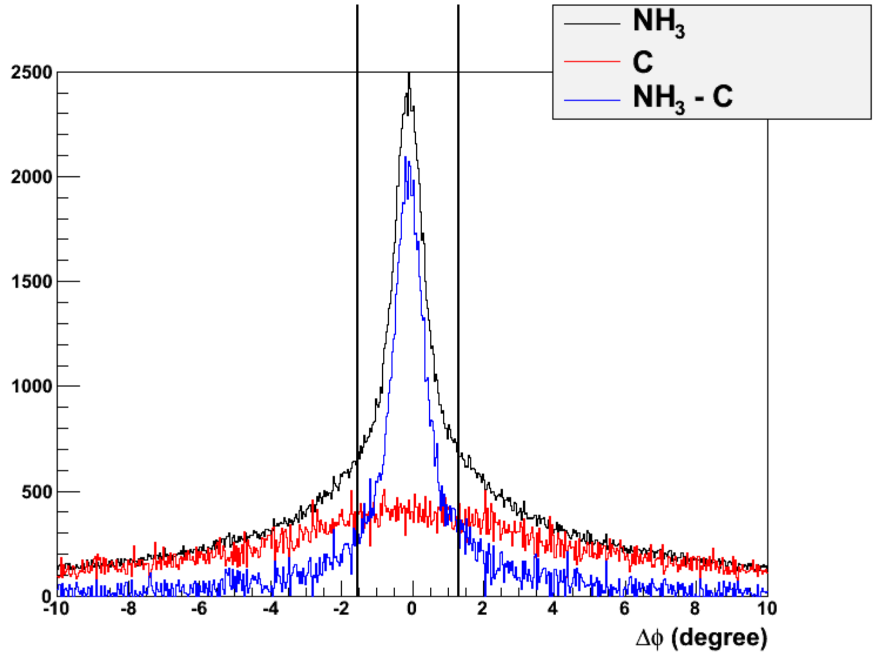

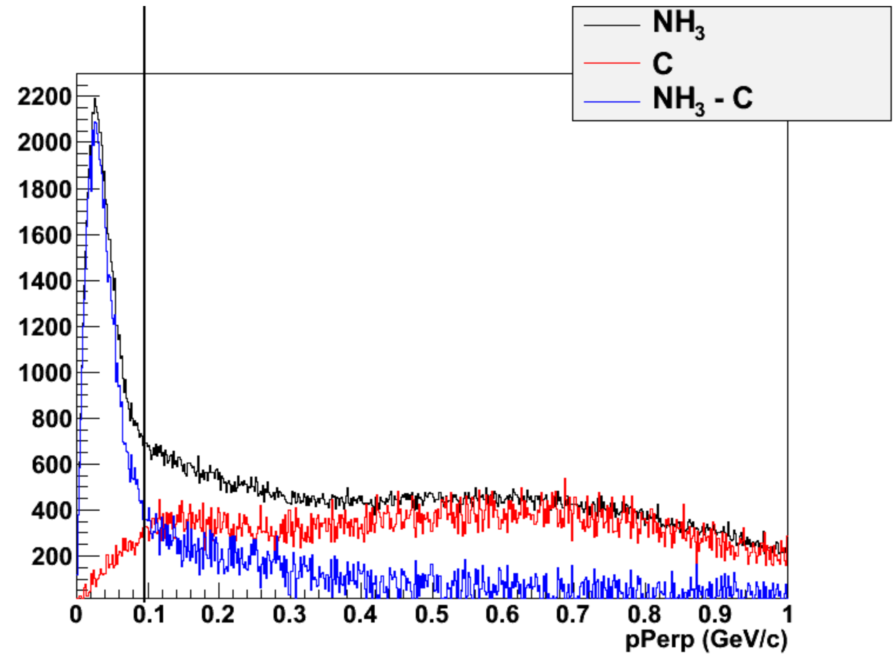

Nuclear background (D_f)

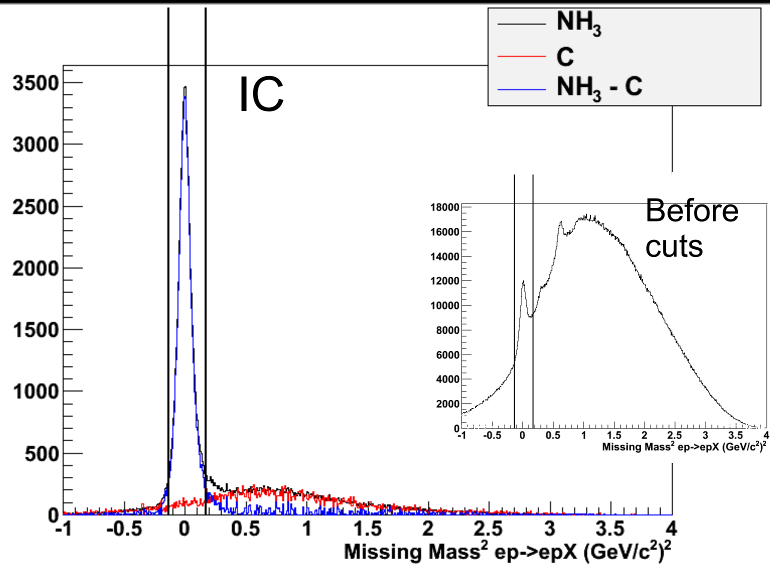

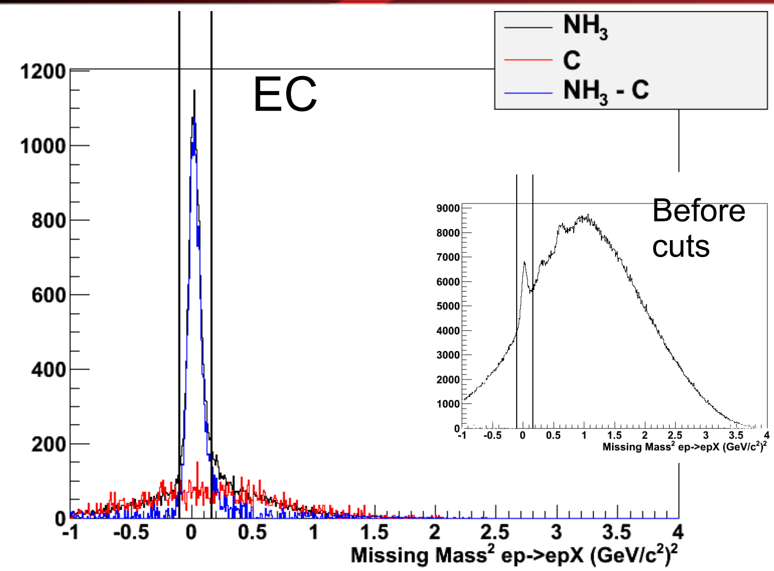

Dilution Factor:

$$D_f = 1 - \frac{N^{C}_{ep\gamma}}{N^{NH_3}_{ep\gamma}}$$

$$A_{UL} = \frac{1}{D_f} \frac{(N^{\downarrow\Uparrow} + N^{\uparrow\Uparrow}) - (N^{\downarrow\Downarrow} + N^{\uparrow\Downarrow})}{(N^{\downarrow\Uparrow} + N^{\uparrow\Uparrow})P^{\Downarrow} + (N^{\downarrow\Downarrow} + N^{\uparrow\Downarrow})P^{\Uparrow}}$$

Part B

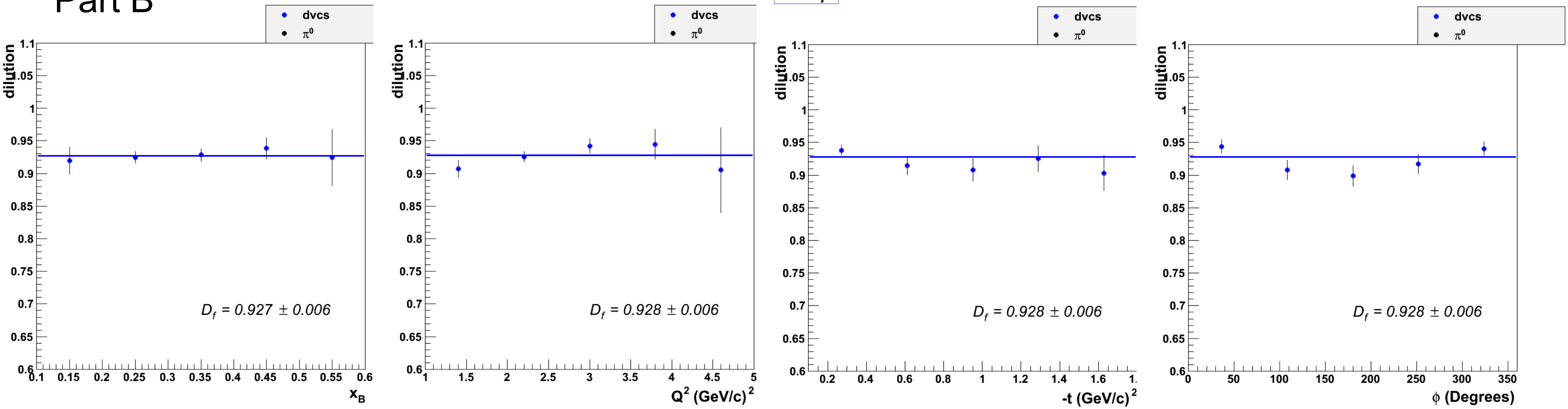

Binning ($e\ p \to e\ p\ \gamma$)

Kinematic bins

$Q^2 = -(p_e - p_e')^2$, $x_B = \dfrac{Q^2}{2m(E_e - E_{e'})}$

$t = (p_p - p_{p'})^2$

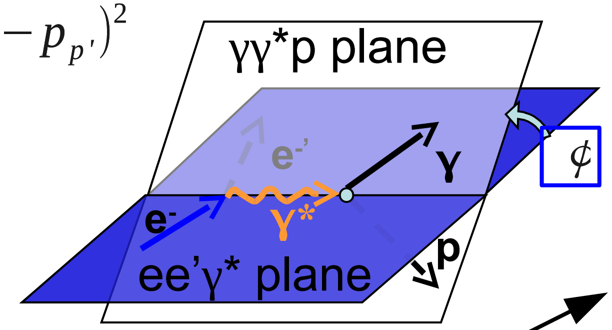

- 5 Bins in Q^2 x_B
- 4 Bins in -t
- 10 Bins in ϕ

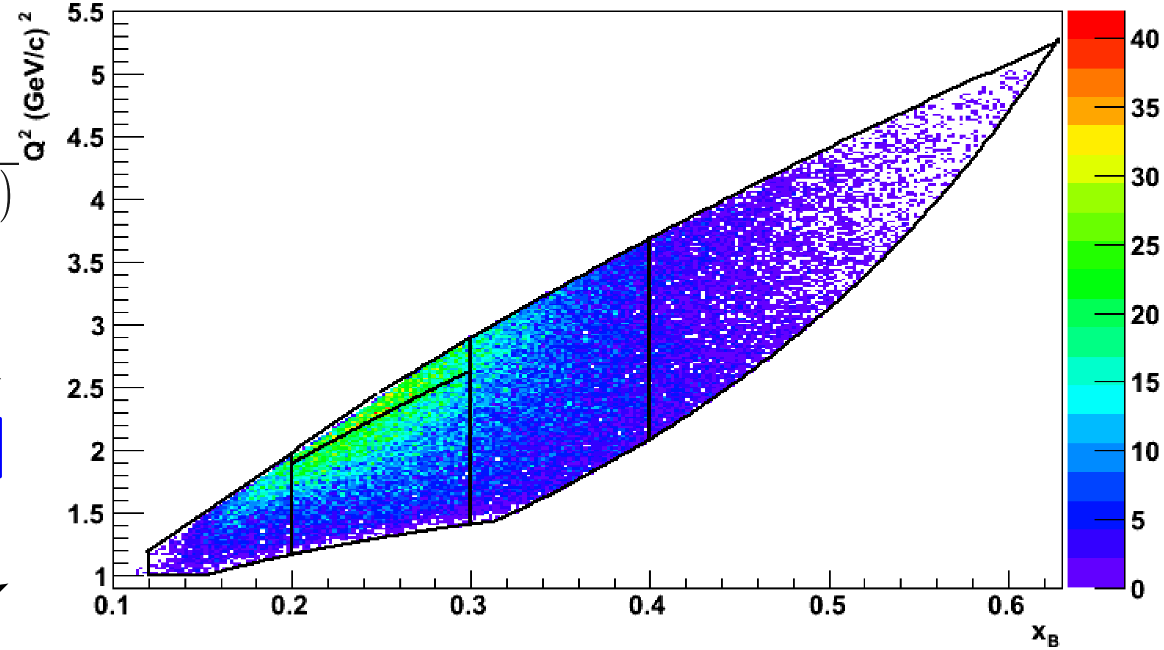

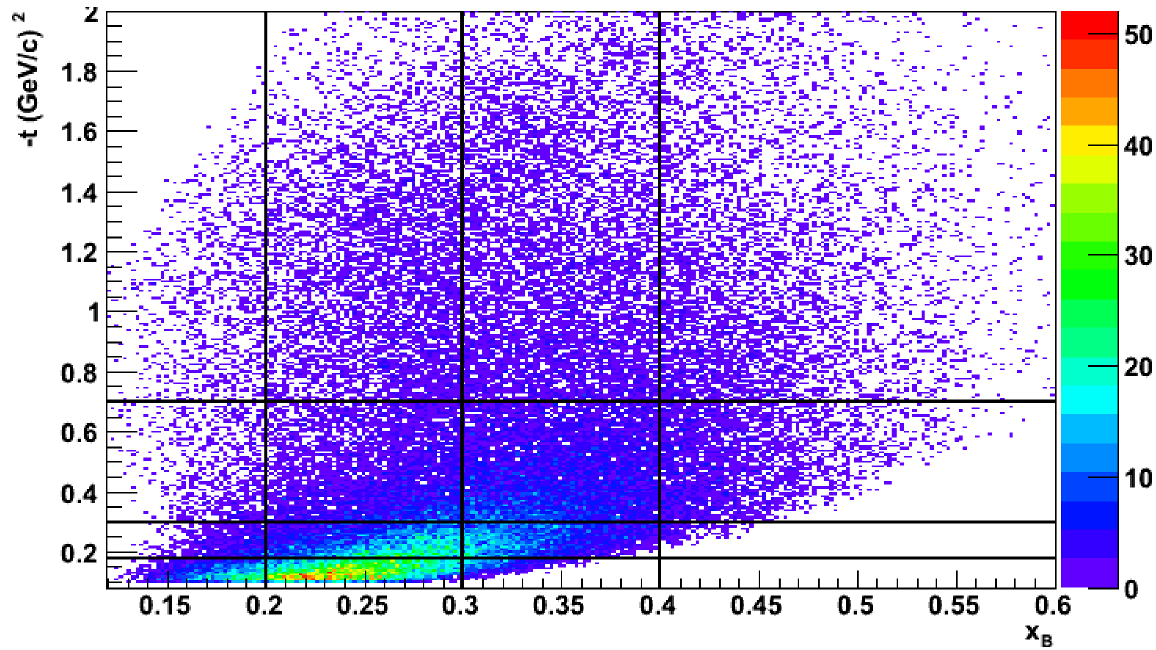

π^0 Contamination

- π^0 electroproduction events where 1 of the π^0 decay photons has sufficiently high energy can reconstruct to appear as a single-photon electroproduction event

- Event selection cuts reduce but not eliminate this contamination to single-photon events

- The fraction of the epγ data which are actually epπ^0 events for each polarization configuration in each kinematic bin is estimated by the correction factor:

$$Bkgr_{\pi^0} = \left(\frac{N_{MC}^{ep\pi^0(\gamma)}}{N_{MC}^{ep\pi^0(\gamma\gamma)}}\right) * \left(\frac{N_{data}^{ep\pi^0}}{N_{data}^{ep\gamma}}\right) * \left(\frac{D_f^{ep\pi^0}}{D_f^{ep\gamma}}\right)$$

Acceptance ratio of single detected photon π^0 events in MC simulation

Ratio of epπ^0 to epγ events in data (scaled by respective nuclear background dilution factors)

- The correction factor is applied on data as:

$$N^{\Downarrow\Uparrow} = (1 - Bkgr_{\pi^0}^{\Downarrow\Uparrow}) \frac{N_{ep\gamma}^{\Downarrow\Uparrow}}{FC^{\Downarrow\Uparrow}}$$

π^0 Contamination

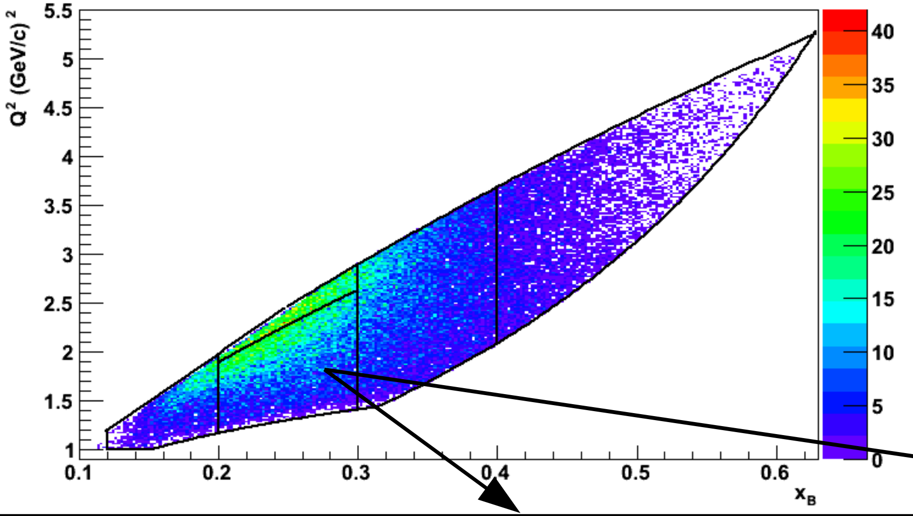

$$Bkgr_{\pi^0} = \left(\frac{N_{MC}^{ep\pi^0(\gamma)}}{N_{MC}^{ep\pi^0(\gamma\gamma)}}\right) * \left(\frac{N_{data}^{ep\pi^0}}{N_{data}^{ep\gamma}}\right) * \left(\frac{D_f^{ep\pi^0}}{D_f^{ep\gamma}}\right)$$

$Bkgr_{\pi^0}$ ranged from

~ 5% at low -t to

~ 30% at higher -t

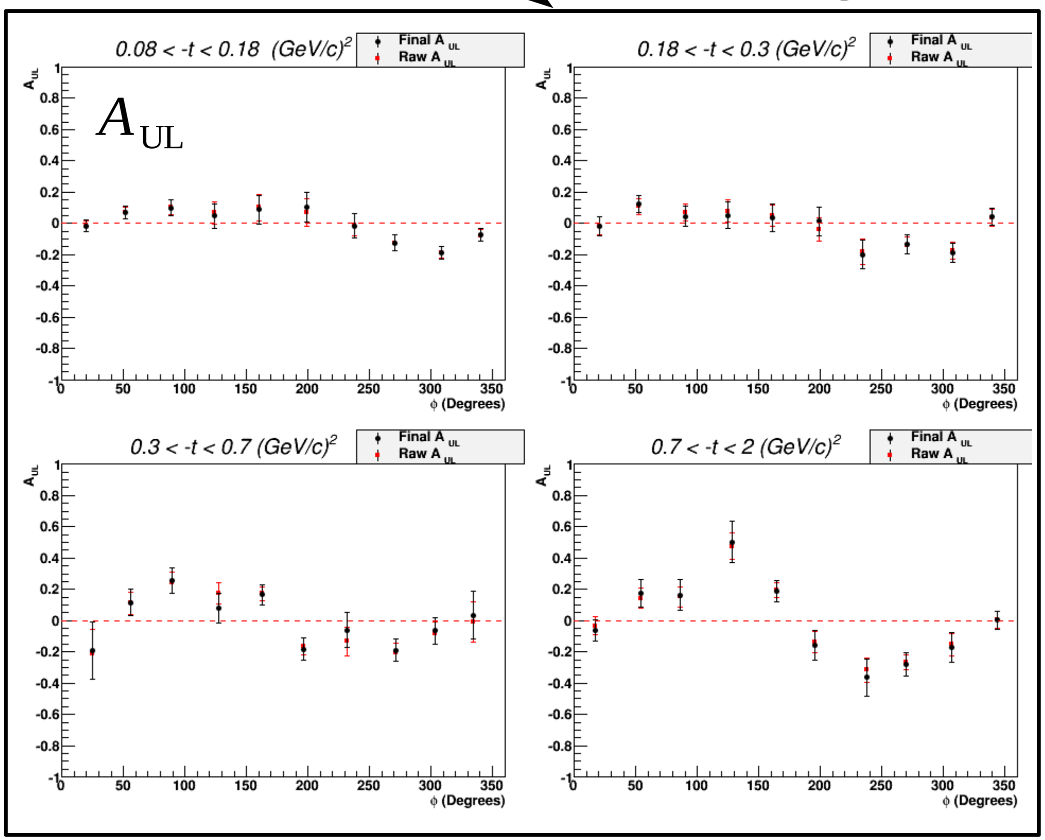

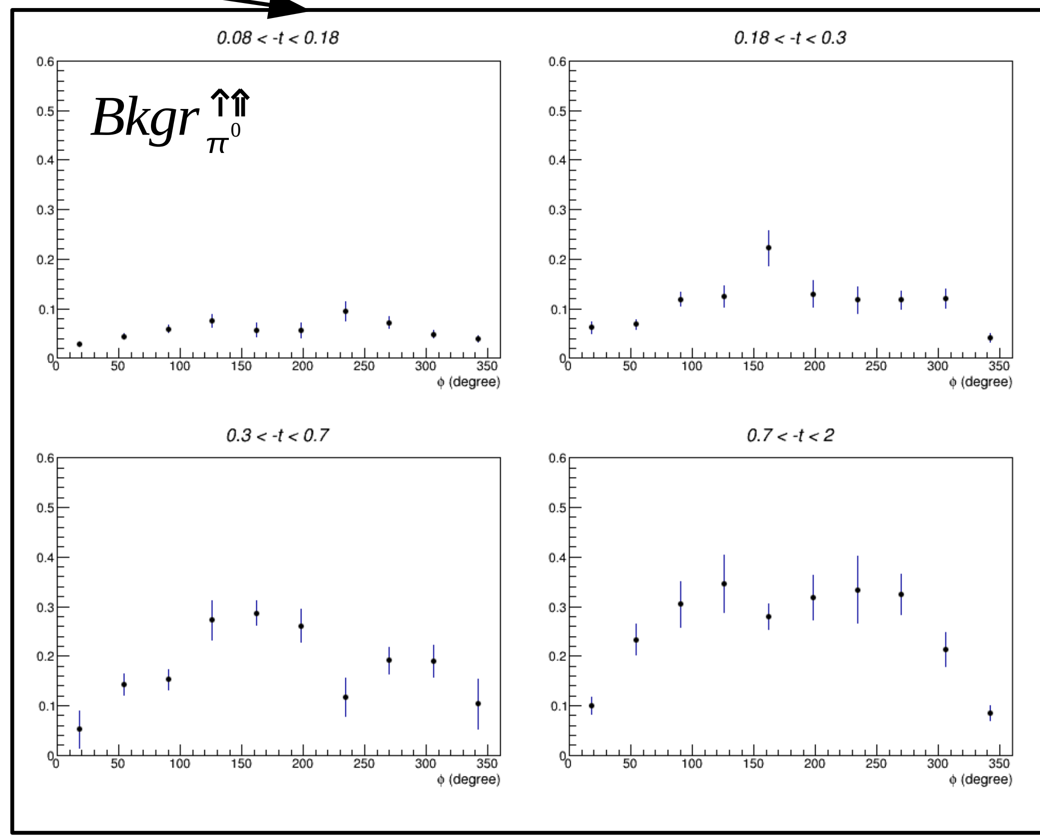

Proton Polarization

Through Elastic Scattering

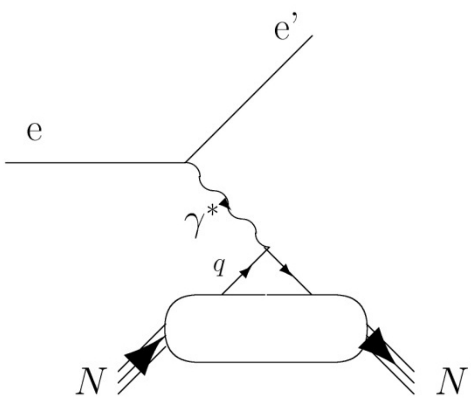

$$A_{\text{meas}} = \frac{1}{D_f}\frac{(N^{\uparrow\Uparrow} - N^{\downarrow\Uparrow})}{(N^{\downarrow\Uparrow} + N^{\uparrow\Uparrow})}$$

$\uparrow / \downarrow$ Electron Helicity State

$\Uparrow / \Downarrow$ Proton Polarization State

$$A_{meas} = (P_b P_t)\ A_{theory}$$

Elastic selection:

$$Q^2 > 1(GeV/c)^2$$

$$0.858 < W < 1.018(GeV/c^2)$$

Mass of the system recoiling against the scattered electron

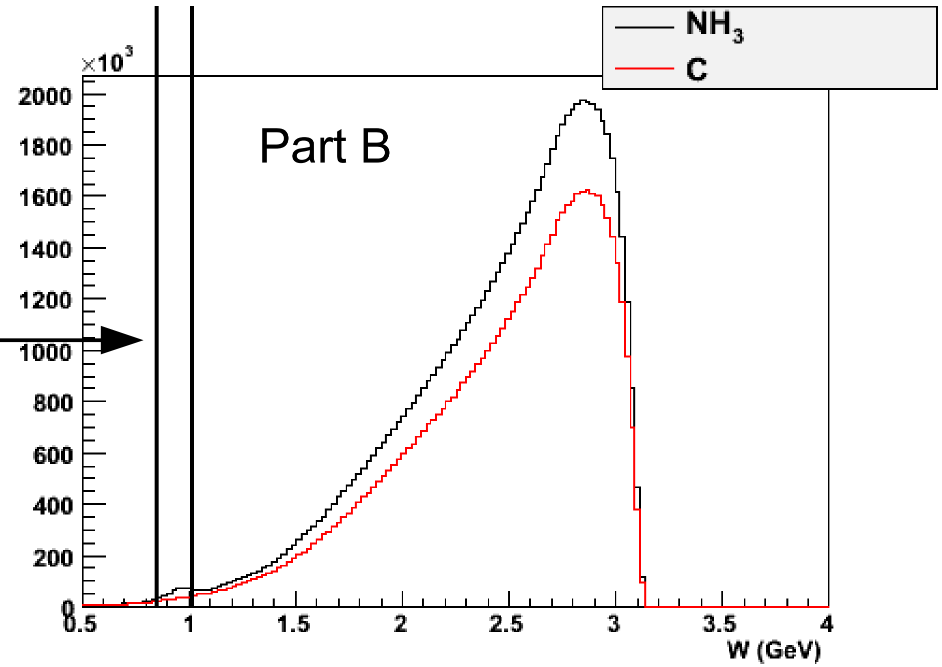

Proton Polarization

Through Elastic Scattering

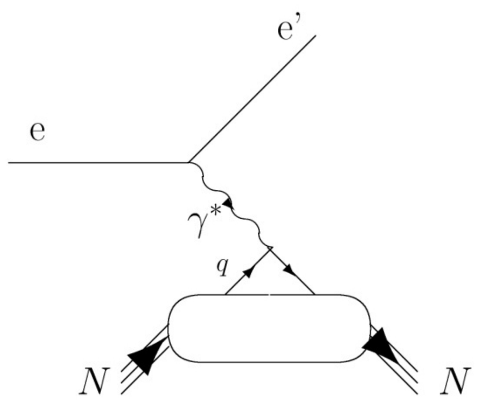

$$A_{\mathrm{meas}} = \frac{1}{D_f}\frac{(N^{\uparrow\Uparrow} - N^{\downarrow\Uparrow})}{(N^{\downarrow\Uparrow} + N^{\uparrow\Uparrow})}$$

$$A_{meas} = (P_b P_t)\ A_{theory}$$

$\uparrow/\downarrow$ Electron Helicity State

$\Uparrow/\Downarrow$ Proton Polarization State

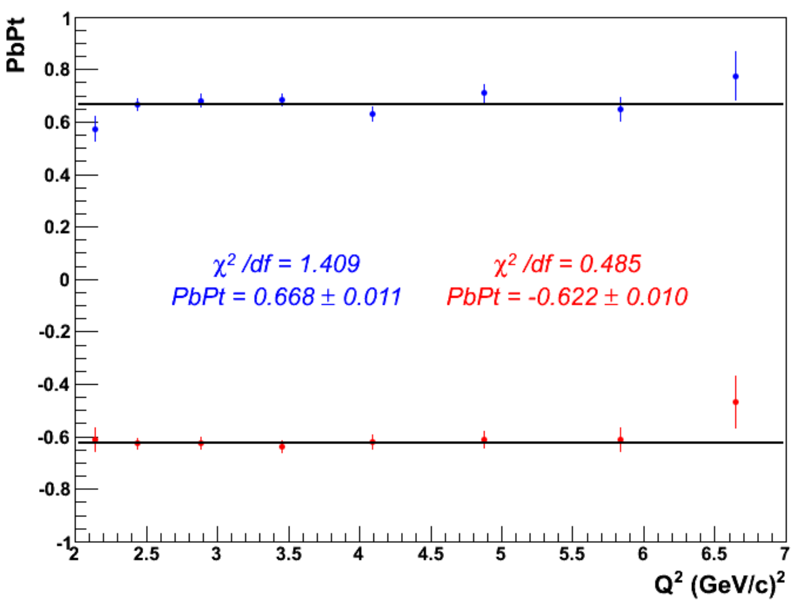

P_b – weighted average of Moller measurements ~ 0.83 (0.02)

Analysis:	elastic	NMR
$P_t^{\Uparrow}$	80 (4) %	78 %
$P_t^{\Downarrow}$	-74 (4) %	-77 %

Transverse Corrections

What we measure and call longitudinal asymmetry is actually, when considered from the virtual- photon perspective, a combination of longitudinal and transverse asymmetries

Applied a model-dependent correction to obtain the TSA and DSA with respect to the virtual photon direction using the relationship[1]:

$$A_{UL}^{\gamma^*} = \frac{A_{UL}}{\cos\theta^*} + \tan\theta^* A_{UT}^{\gamma^*}(\phi_S = 0)$$

The x-component of the transverse asymmetry (estimated with VGG)

The angle formed by the virtual photon and the beam direction

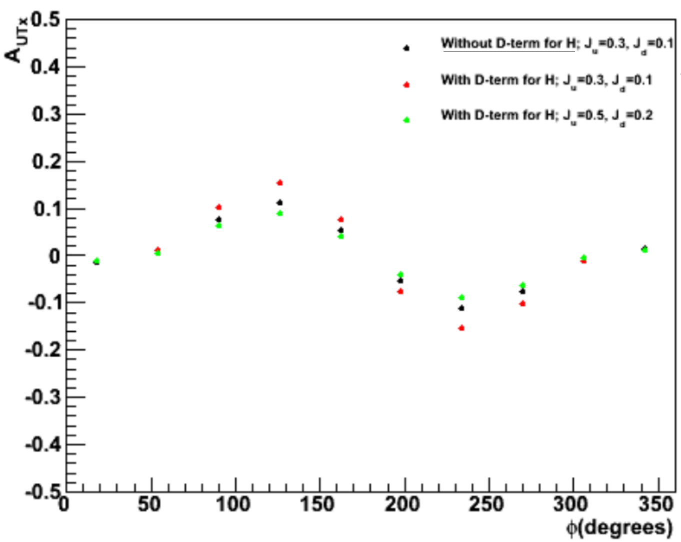

Relatively small transverse asymmetry and small angle gives overall a very small effect:

$\langle Q^2\rangle$ =1.97 GeV^2 ,$\langle x_B\rangle$ = 0.256

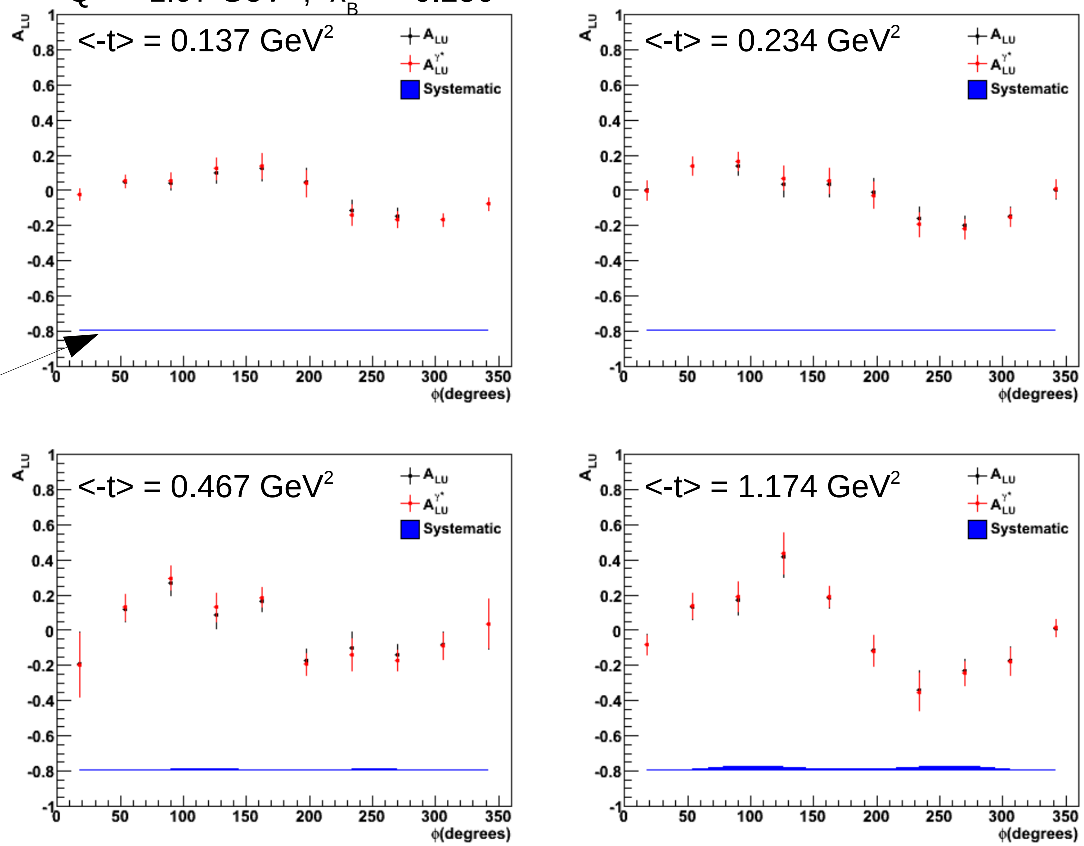

[1] M. Diehl and S. Sapeta, Eur. Phys. J. C41, 515 (2005).

Systematics

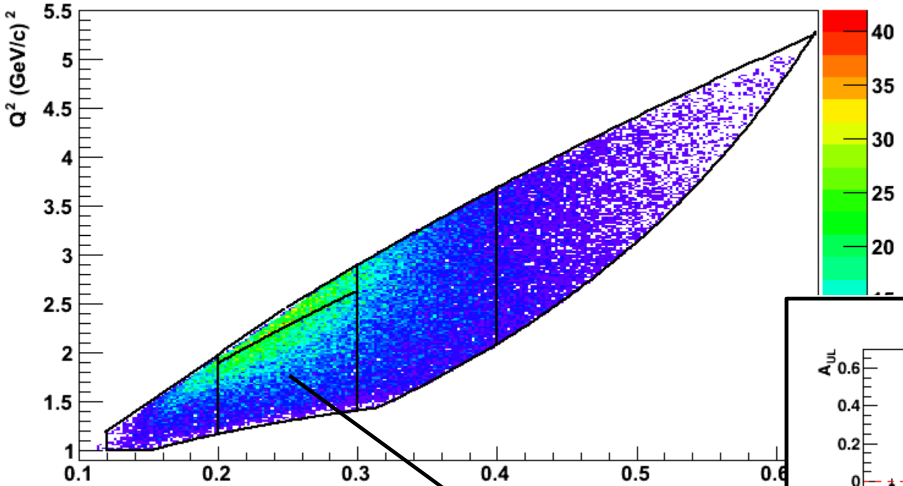

Target Spin Asymmetry (TSA)

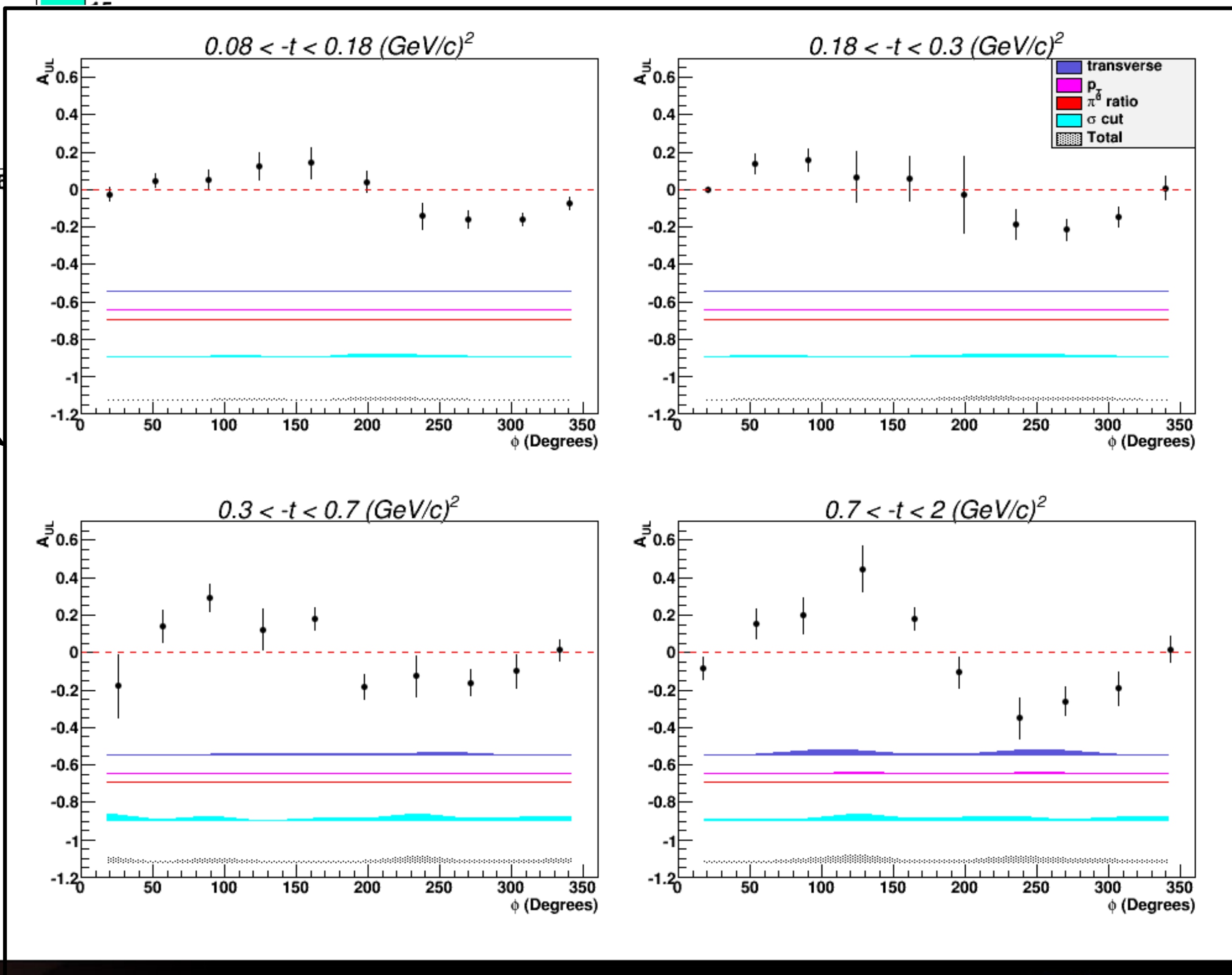

	Source
1	Transverse corrections
2	P_bP_t, P_b, P_t
3	$ep\pi^0$ background subtraction
4	DVCS exclusivity cuts

$$\Delta_{RMS} = \frac{\sqrt{\Sigma_x \Delta_x^2}}{\sqrt{N}}$$

Beam-Spin Asymmetry

$$A_{LU} = \frac{1}{P_B} \frac{(N^{\uparrow\Uparrow} - N^{\downarrow\Uparrow})P^{\Downarrow} + (N^{\uparrow\Downarrow} - N^{\downarrow\Downarrow})P^{\Uparrow}}{(N^{\downarrow\Uparrow} + N^{\uparrow\Uparrow})P^{\Downarrow} + (N^{\downarrow\Downarrow} + N^{\uparrow\Downarrow})P^{\Uparrow}}$$

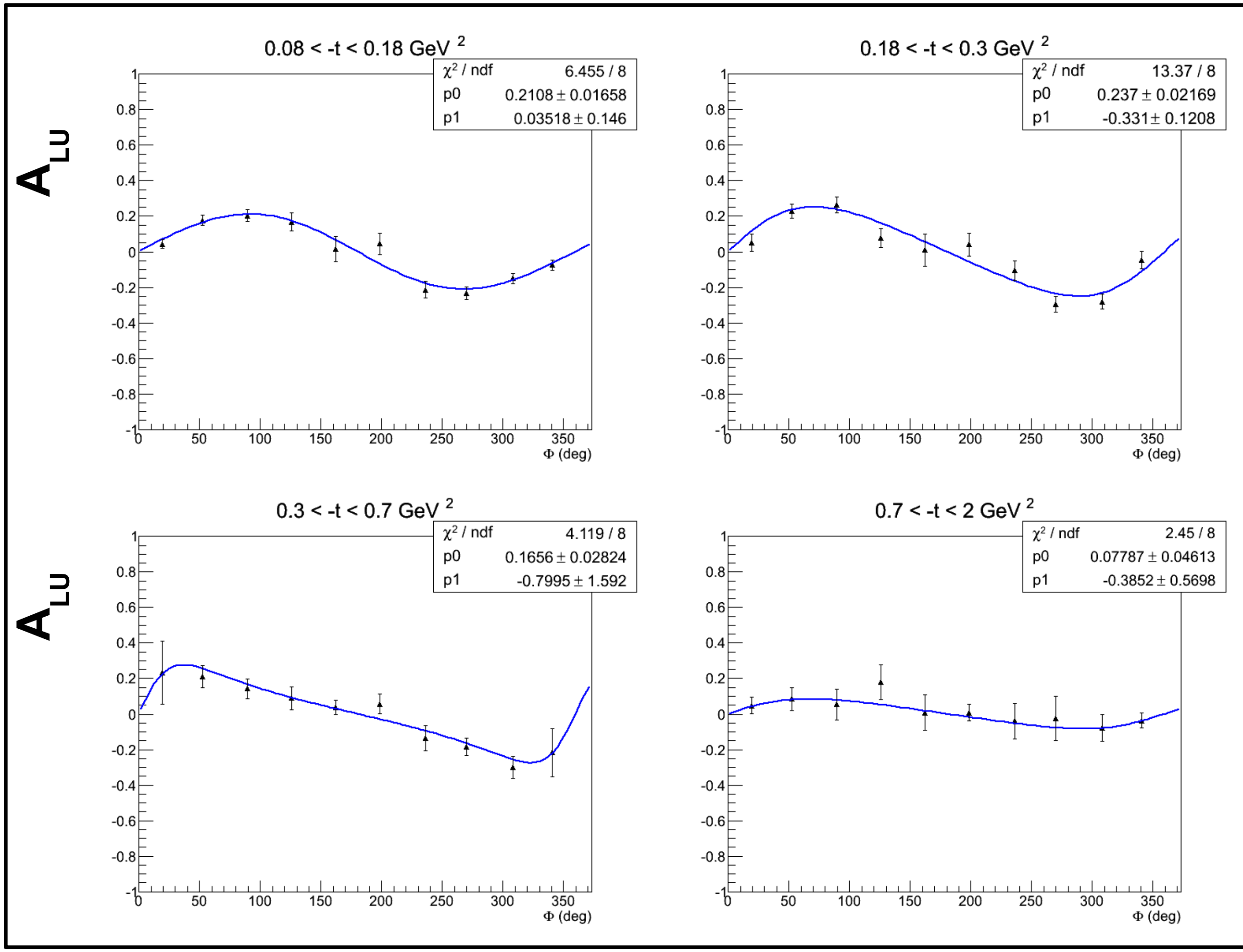

Kinematic bins

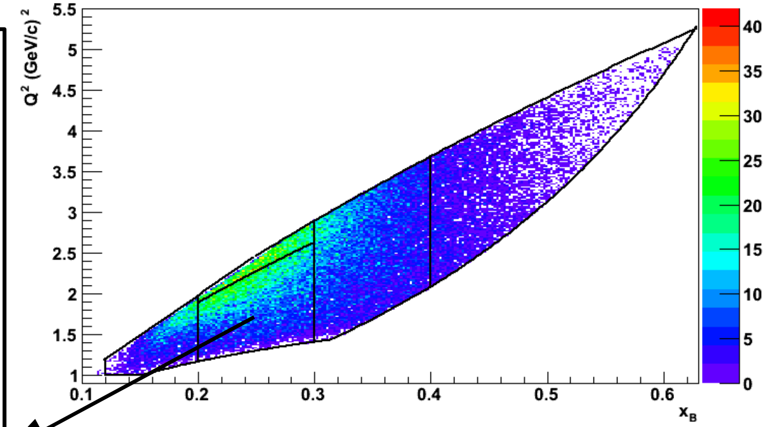

$$Q^2 = -(\boldsymbol{p}_e - \boldsymbol{p}_e')^2$$

$$x_B = \frac{Q^2}{2m(E_e - E_{e'})}$$

$$t = (\boldsymbol{p}_p - \boldsymbol{p}_{p'})^2$$

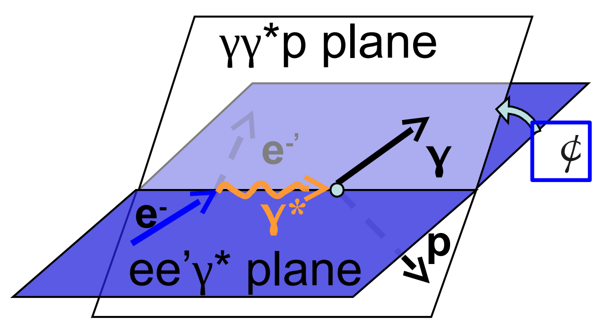

Fit Function: $\frac{[2]\sin\phi}{1+[1]\cos\phi}$

Beam-Spin Asymmetry

Comparison with Existing Data

Fit Function: $\dfrac{[2]\sin\phi}{1+[1]\cos\phi}$

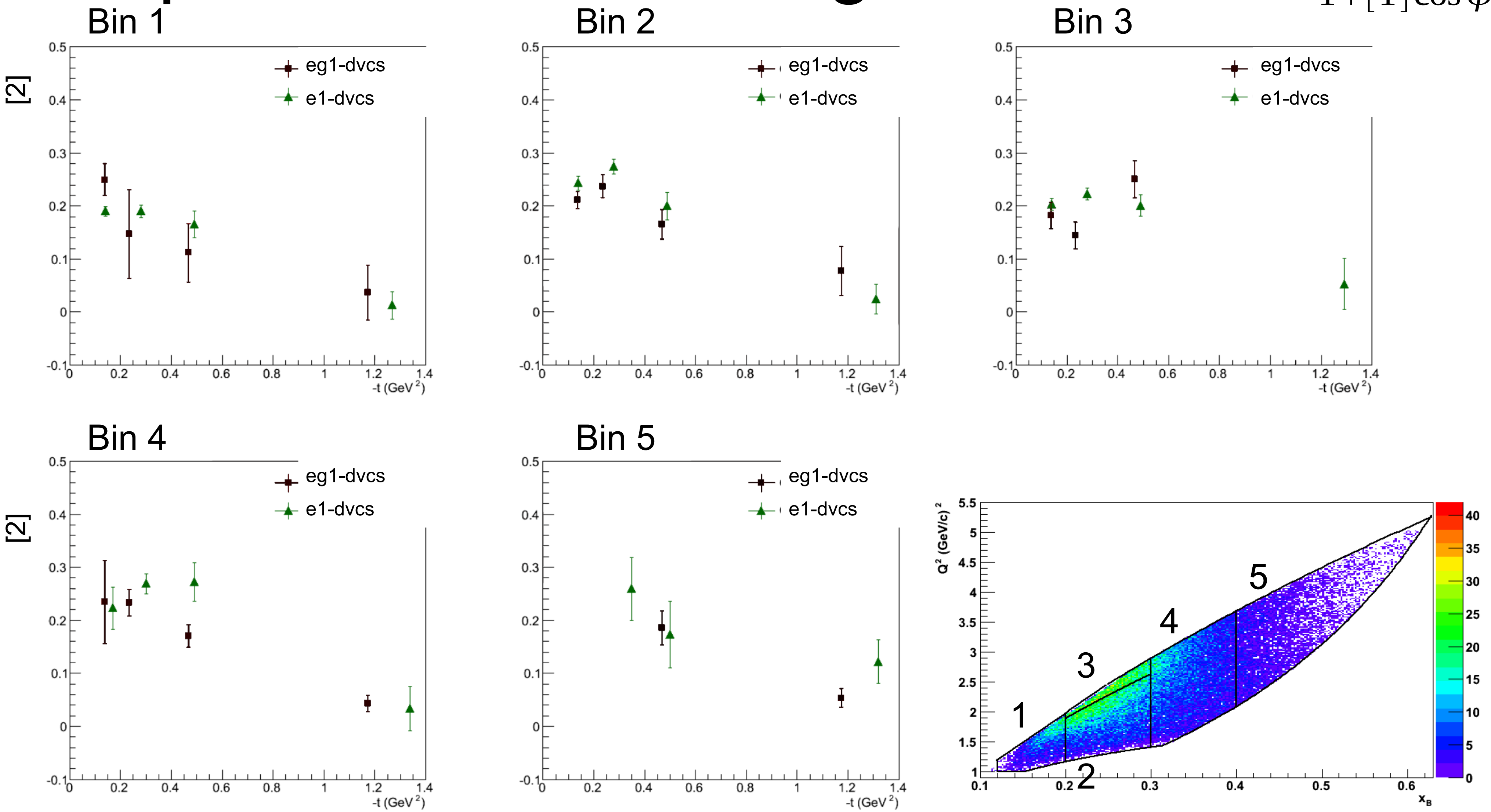

Double-Spin Asymmetry

$$A_{\mathrm{LL}} = \frac{1}{P_B D_f}\frac{(N^{\uparrow\Uparrow}+N^{\downarrow\Downarrow}) - (N^{\uparrow\Downarrow}+N^{\downarrow\Uparrow})}{(N^{\downarrow\Uparrow}+N^{\uparrow\Uparrow})P^{\Downarrow} + (N^{\downarrow\Downarrow}+N^{\uparrow\Downarrow})P^{\Uparrow}}$$

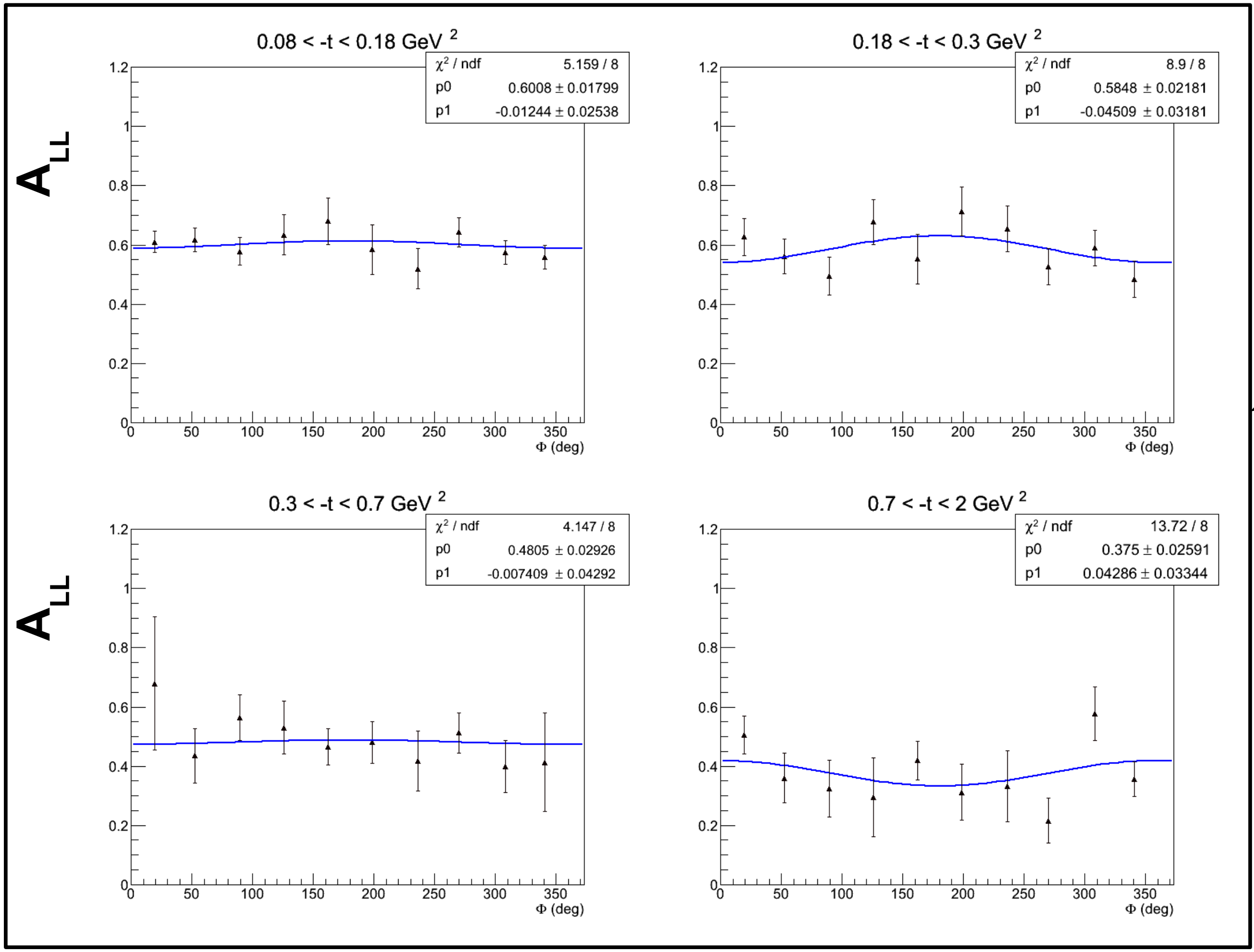

Kinematic bins

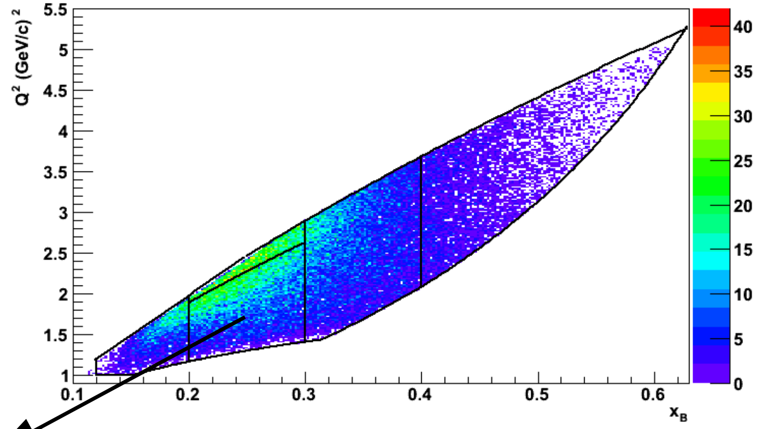

$$Q^2 = -(\boldsymbol{p_e} - \boldsymbol{p_e}')^2$$

$$x_B = \frac{Q^2}{2m(E_e - E_{e'})}$$

$$t = (\boldsymbol{p_p} - \boldsymbol{p_{p'}})^2$$

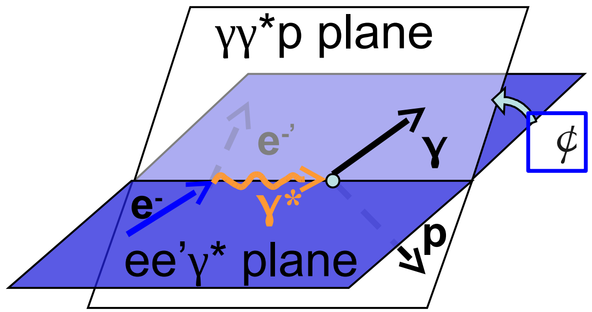

Fit Function: $[1]+[2]\cos\phi$

Double-Spin Asymmetry

Kinematic dependence

Fit Function: $\underline{[1]}+[2]\cos\phi$

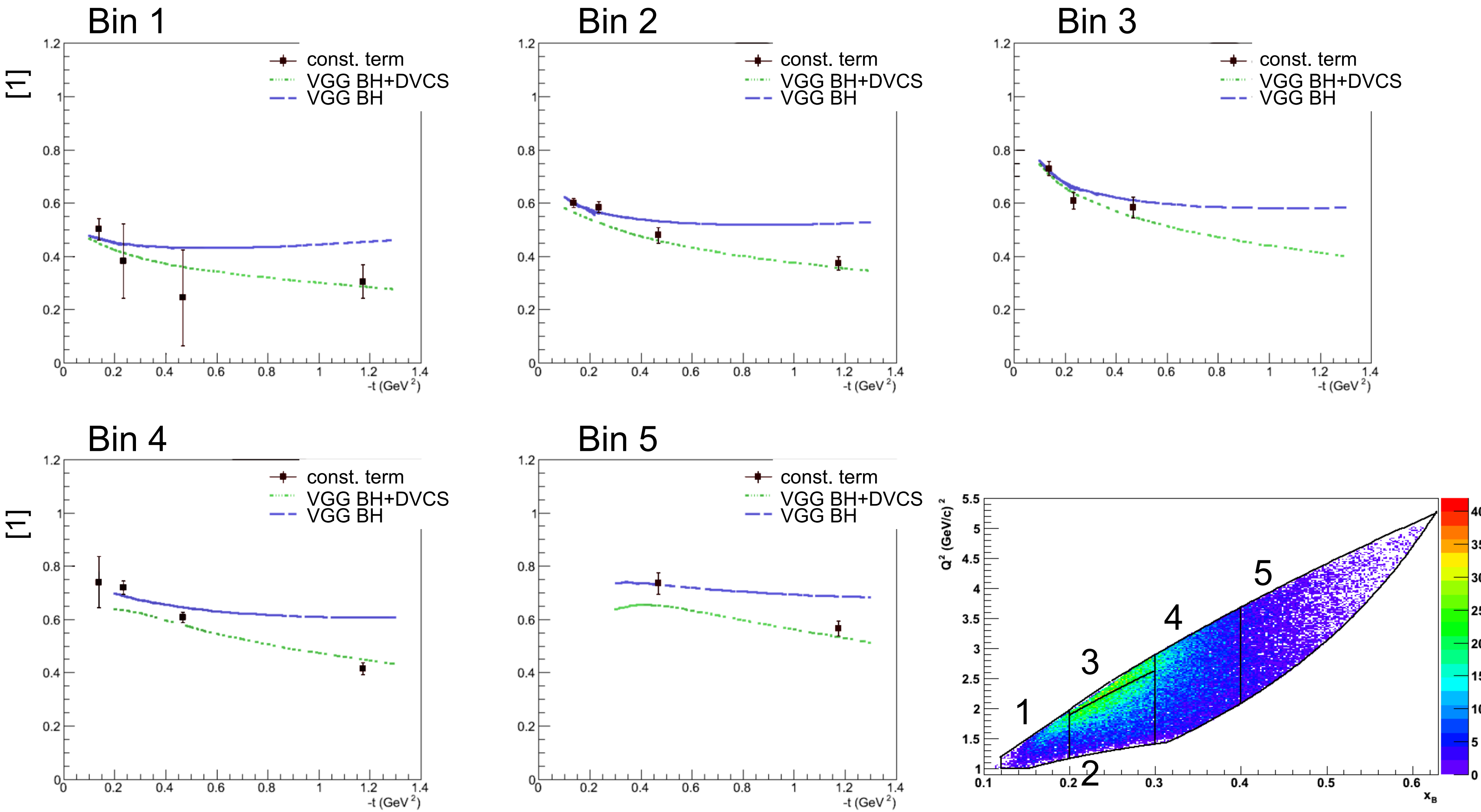

Double-Spin Asymmetry

Kinematic dependence

Fit Function: $[1]+\underline{[2]}\cos\phi$

Bin 1

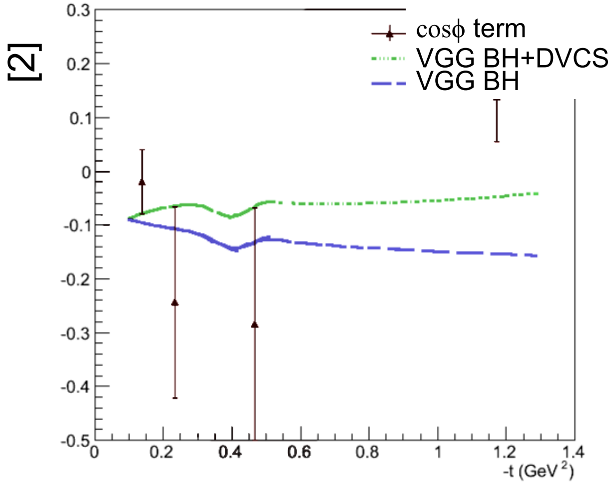

Bin 2

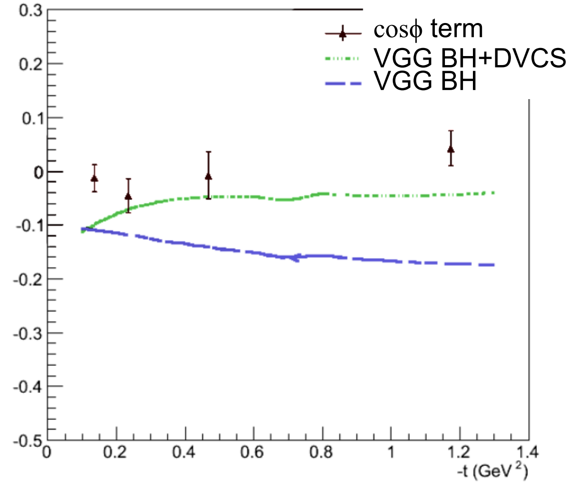

Bin 3

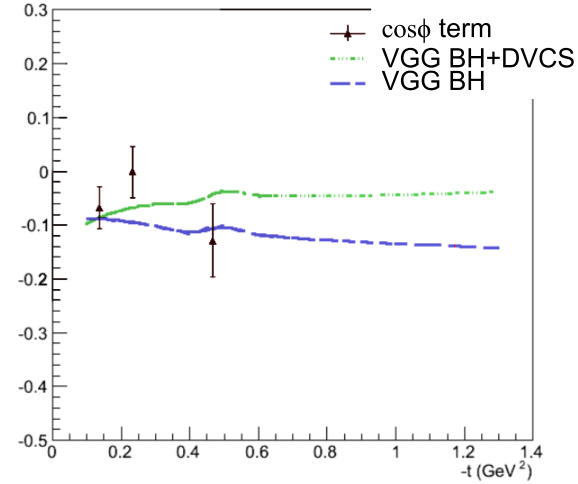

Bin 4

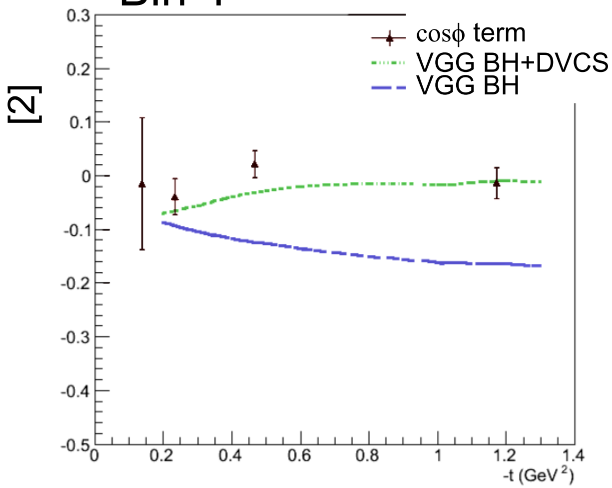

Bin 5

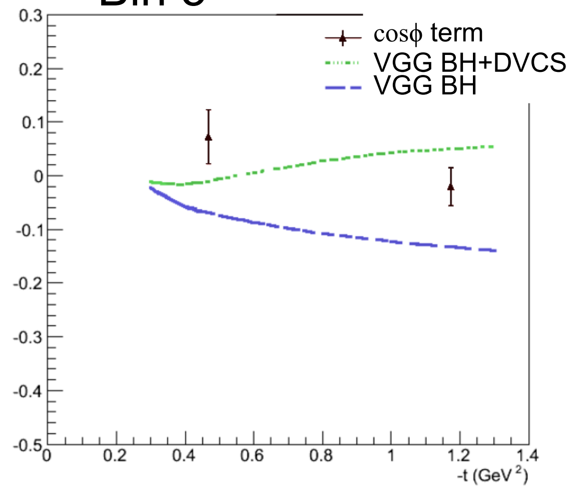

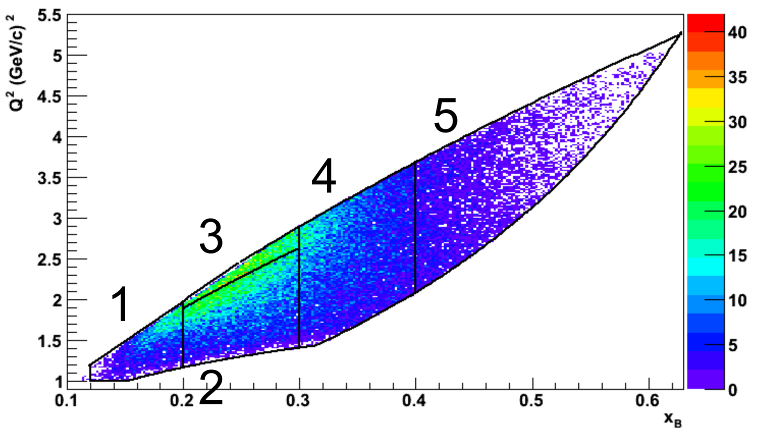

Target-Spin Asymmetry

$$A_{UL} = \frac{1}{D_f}\,\frac{\left(N^{\downarrow\Uparrow}+N^{\uparrow\Uparrow}\right)-\left(N^{\downarrow\Downarrow}+N^{\uparrow\Downarrow}\right)}{\left(N^{\downarrow\Uparrow}+N^{\uparrow\Uparrow}\right)P^{\Downarrow}+\left(N^{\downarrow\Downarrow}+N^{\uparrow\Downarrow}\right)P^{\Uparrow}}$$

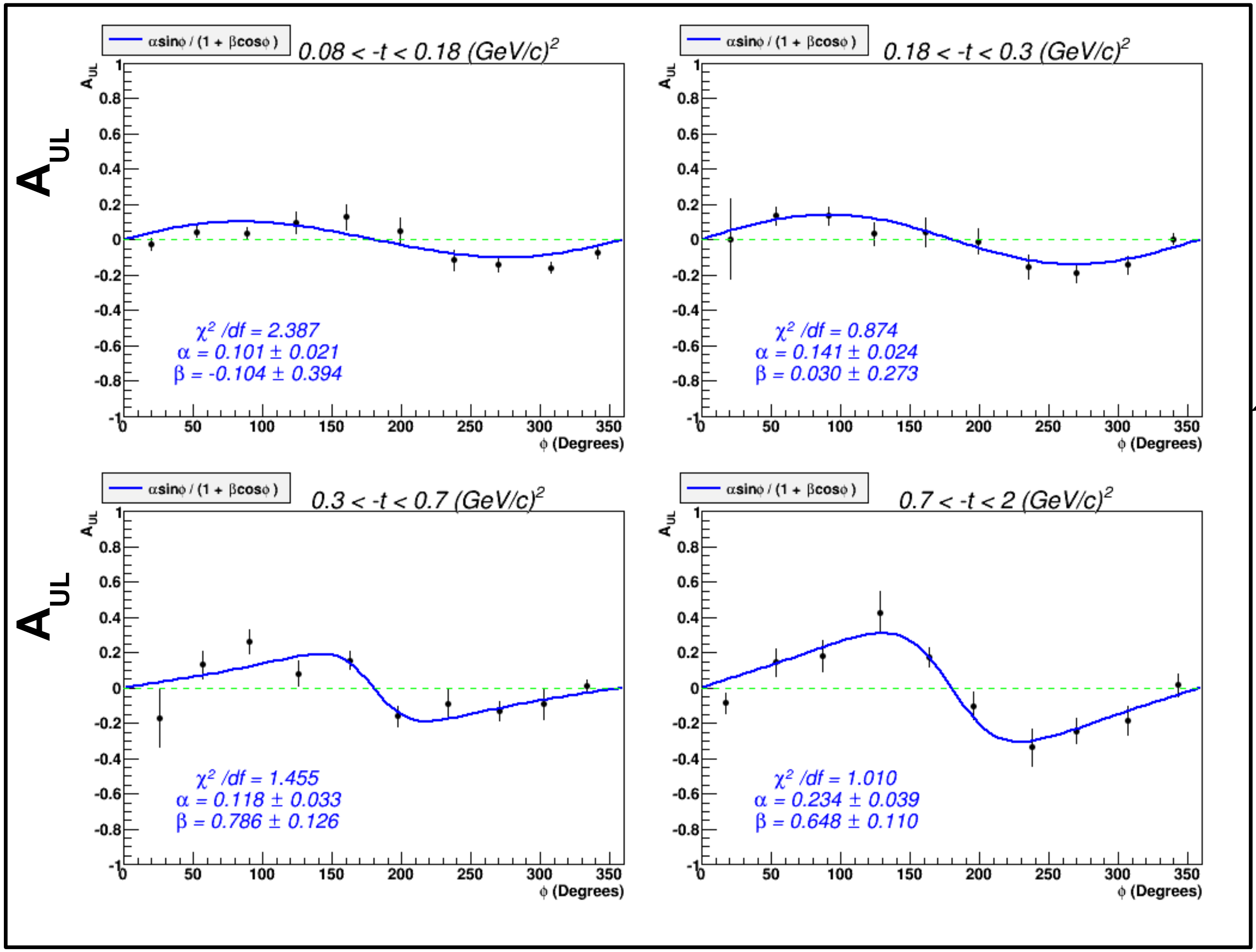

Kinematic bins

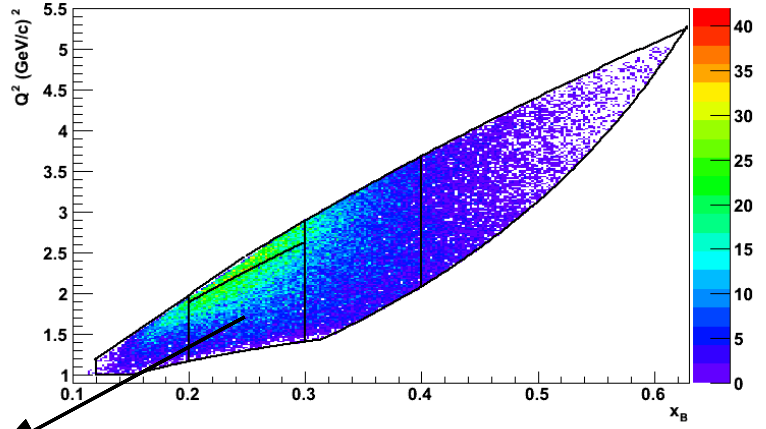

$$Q^2 = -(p_e - p_e{}')^2$$

$$x_B = \frac{Q^2}{2m(E_e - E_{e'})}$$

$$t = (p_p - p_{p'})^2$$

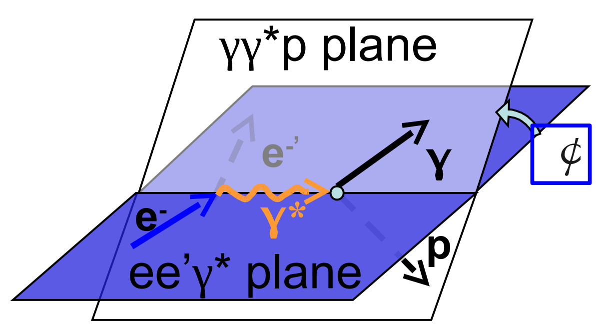

Fit Function: $\frac{[2]\sin\phi}{1+[1]\cos\phi}$

Target-Spin Asymmetry

Kinematic dependence

Fit Function: $\frac{[2]\sin\phi}{1+[1]\cos\phi}$

Bin 1

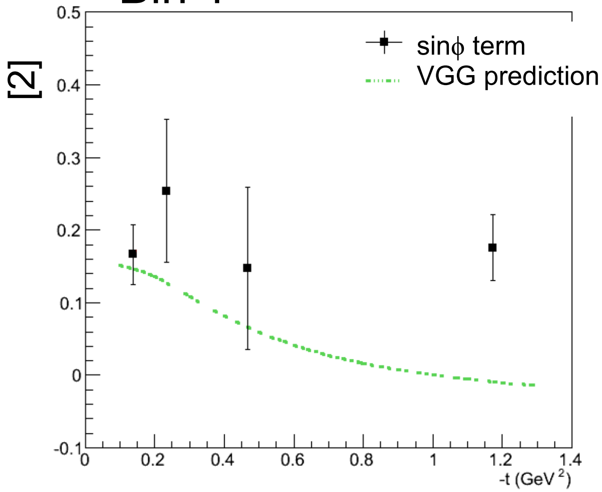

Bin 2

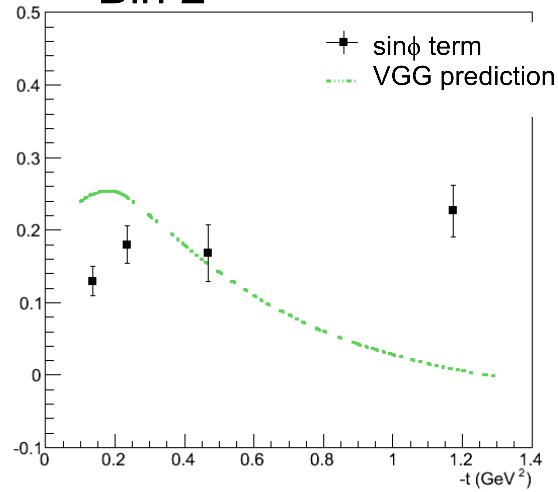

Bin 3

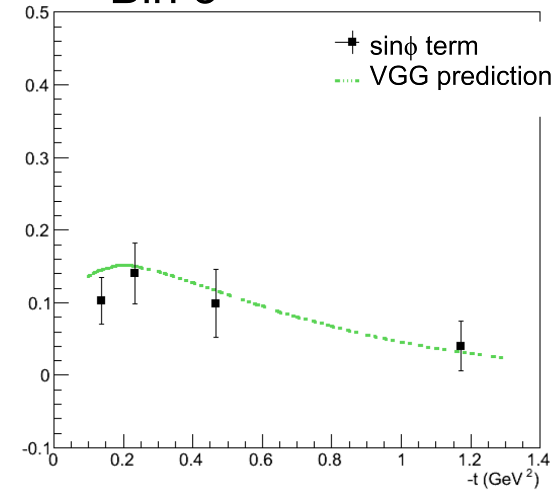

Bin 4

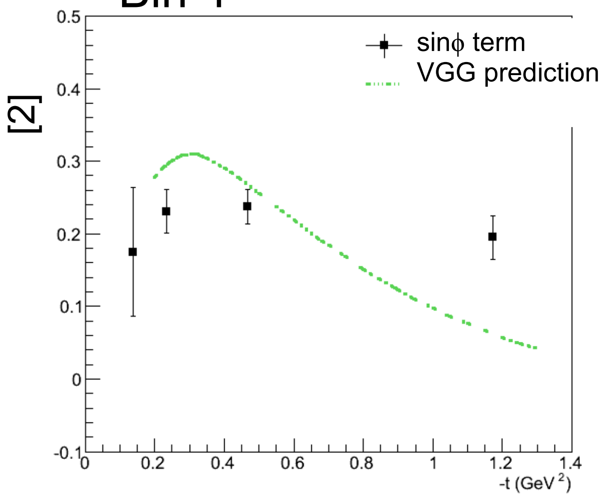

Bin 5

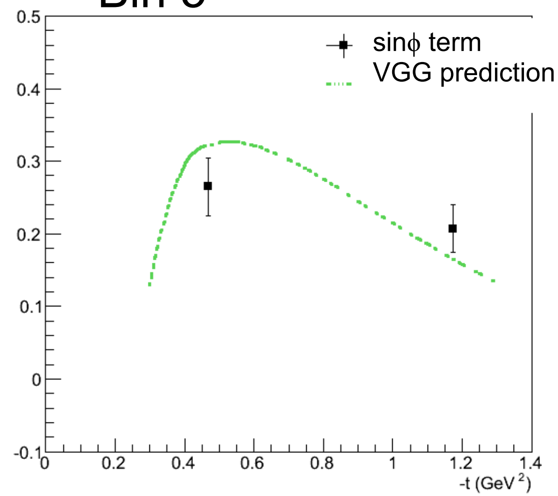

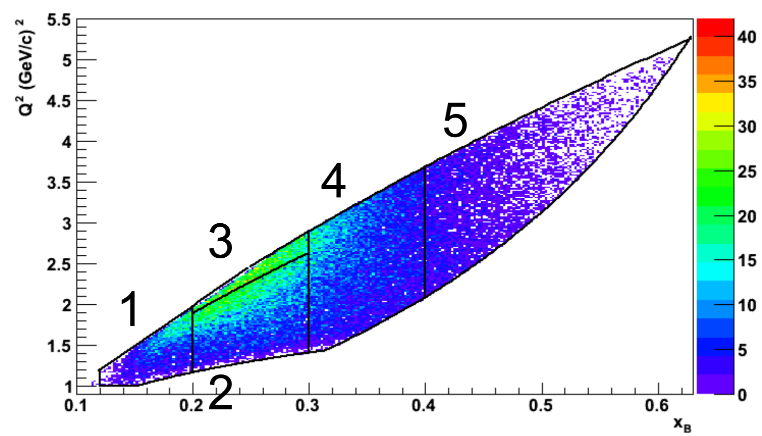

Comparison with Existing Data

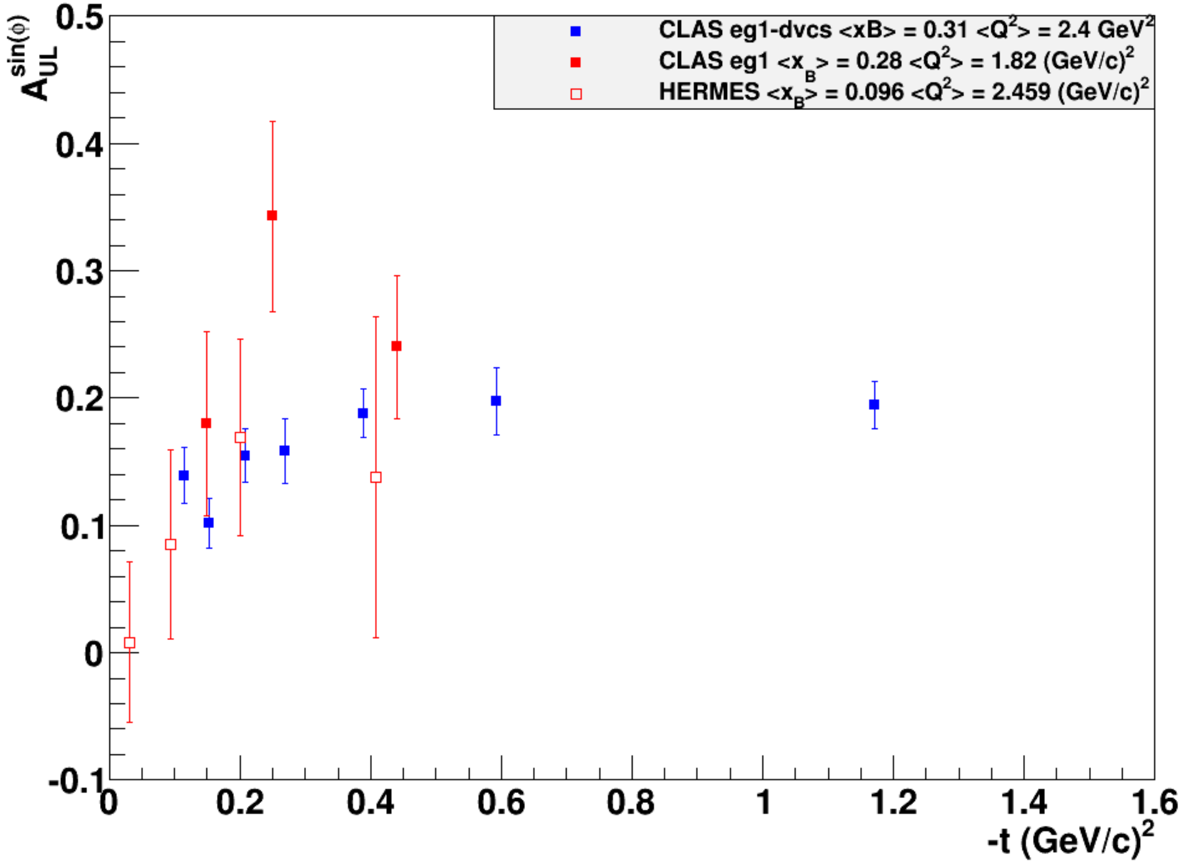

Multi-Fit for Higher Order Extraction

$$A_{UL}: \frac{[2]\sin\phi + [3]\sin 2\phi}{1+[1]\cos\phi}$$

Limited statistical precision and small number of bins in
=> ambiguous conclusions about higher order functional dependence

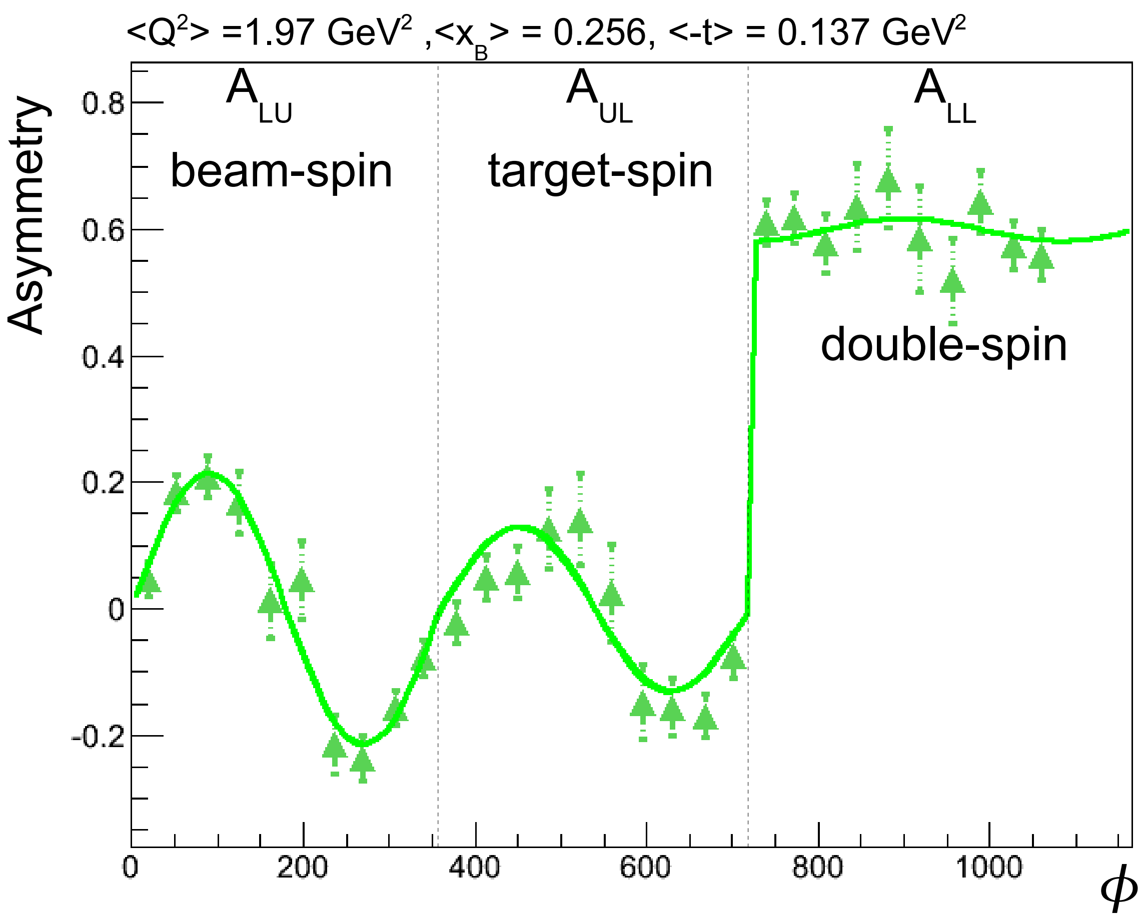

$$A_{LU}: \frac{[0]\sin\phi}{1+[1]\cos\phi}$$

$$A_{UL}: \frac{[2]\sin\phi + [3]\sin 2\phi}{1+[1]\cos\phi}$$

$$A_{LL}: \frac{[4]+[5]\cos\phi}{1+[1]\cos\phi}$$

Common parameter

Multi-Fit for Higher Order Extraction

$$A_{UL}: \frac{[2]\sin\phi + [3]\sin 2\phi}{1+[1]\cos\phi}$$

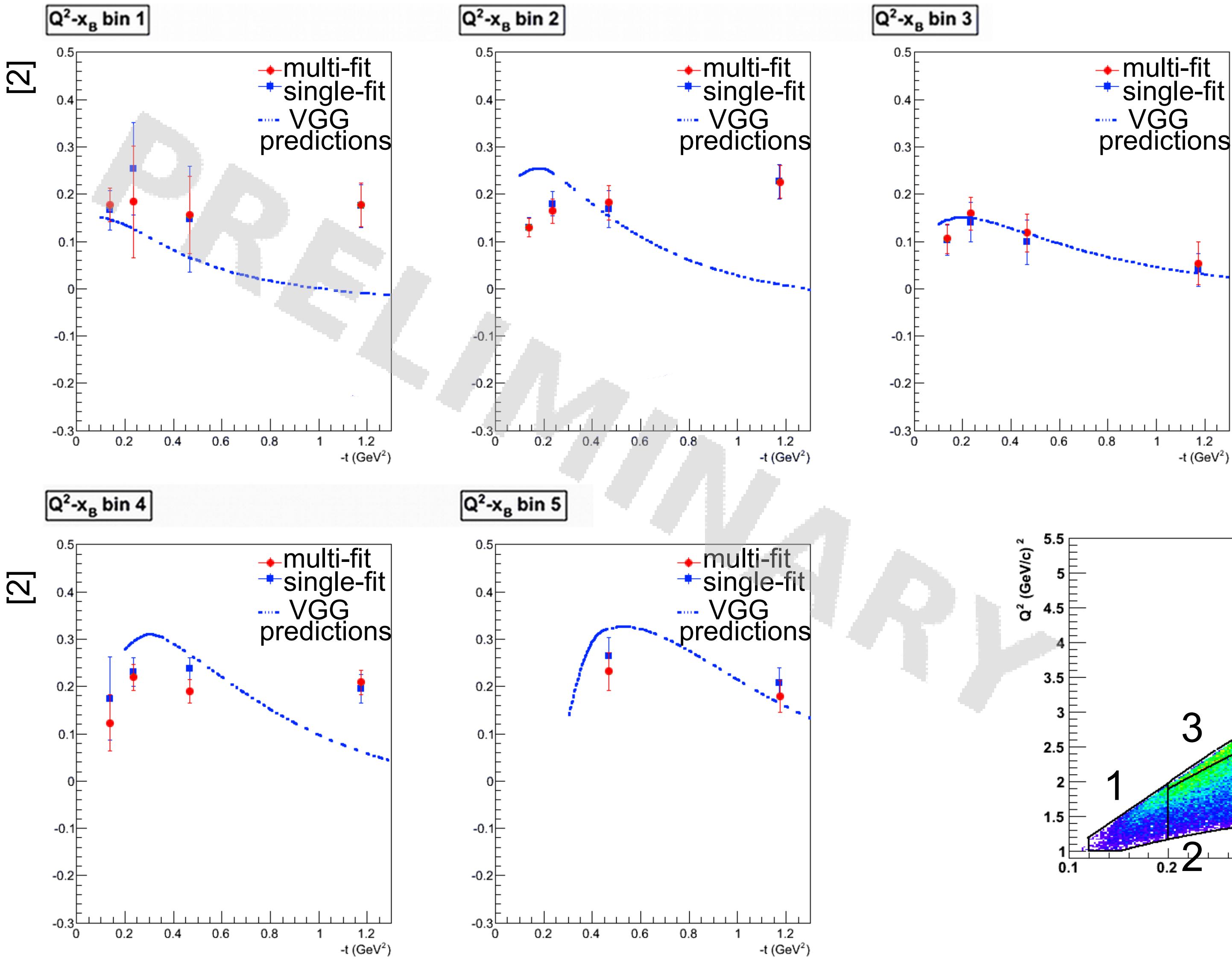

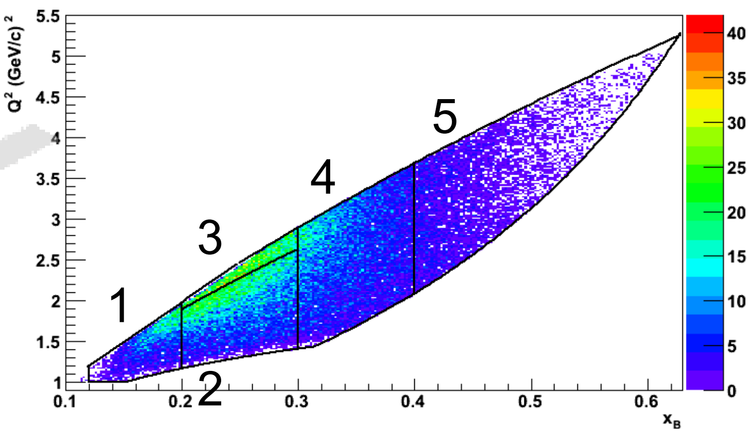

Multi-Fit for Higher Order Extraction

$$A_{UL}: \frac{[2]\sin\phi + [3]\sin 2\phi}{1+[1]\cos\phi}$$

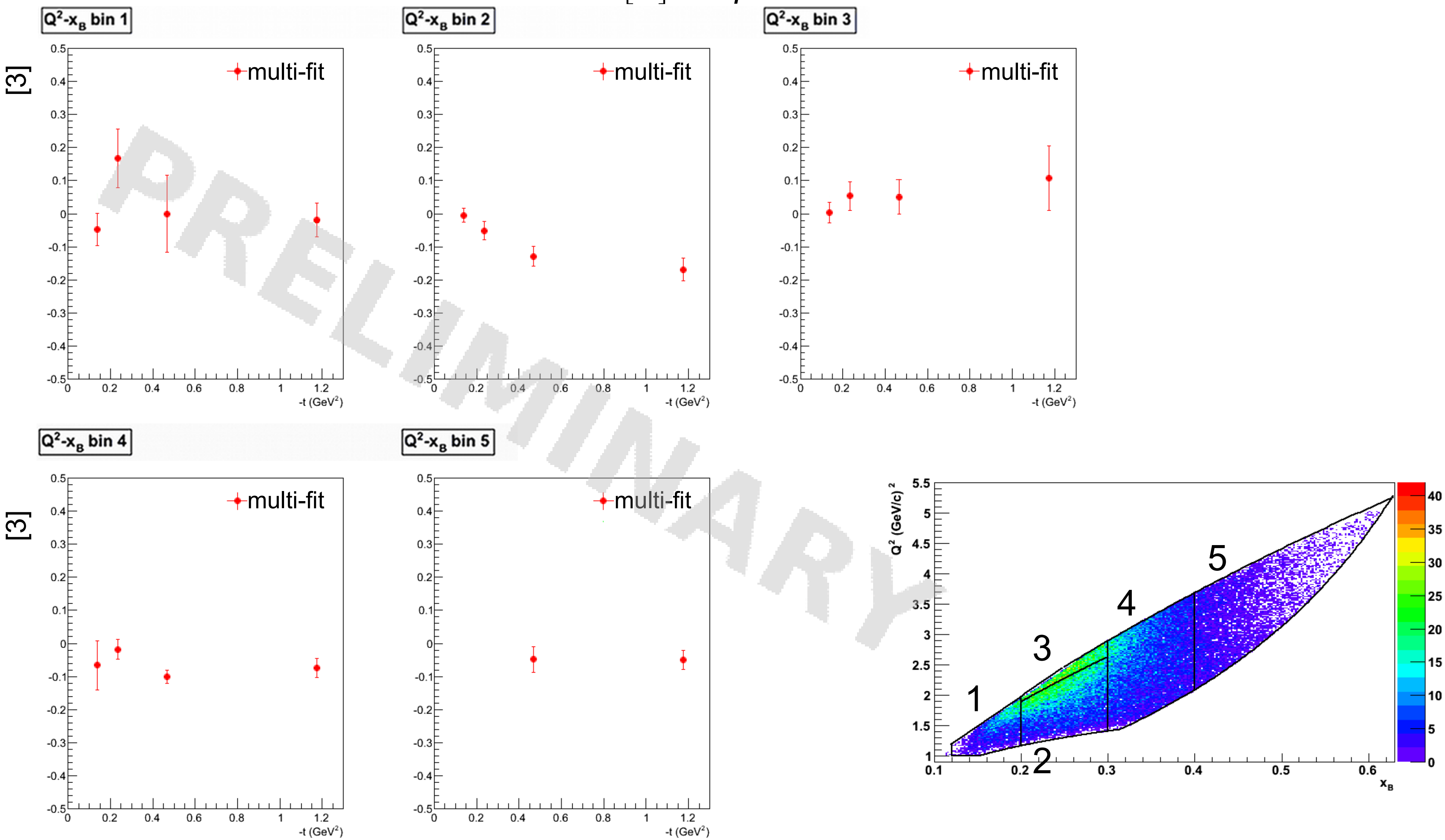

CFF Extraction

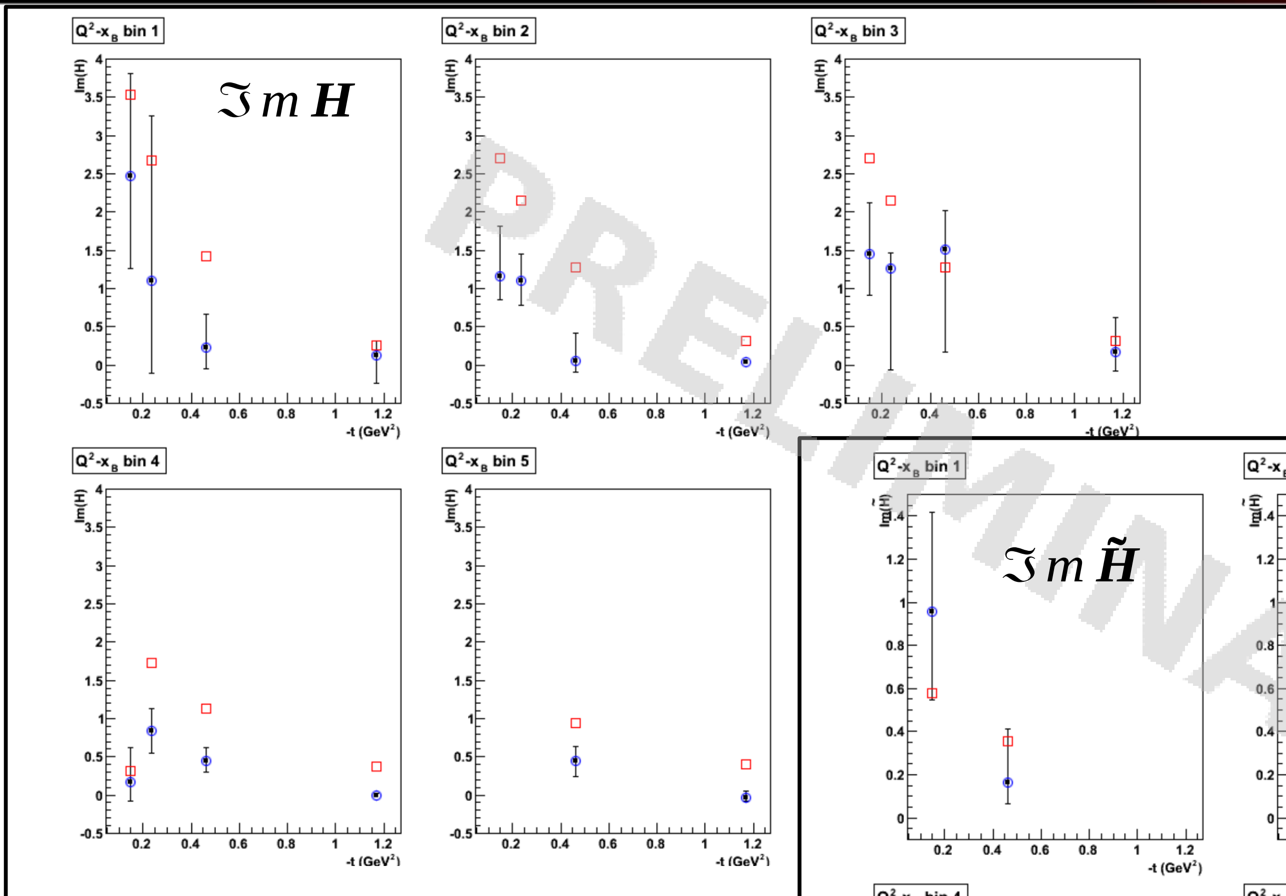

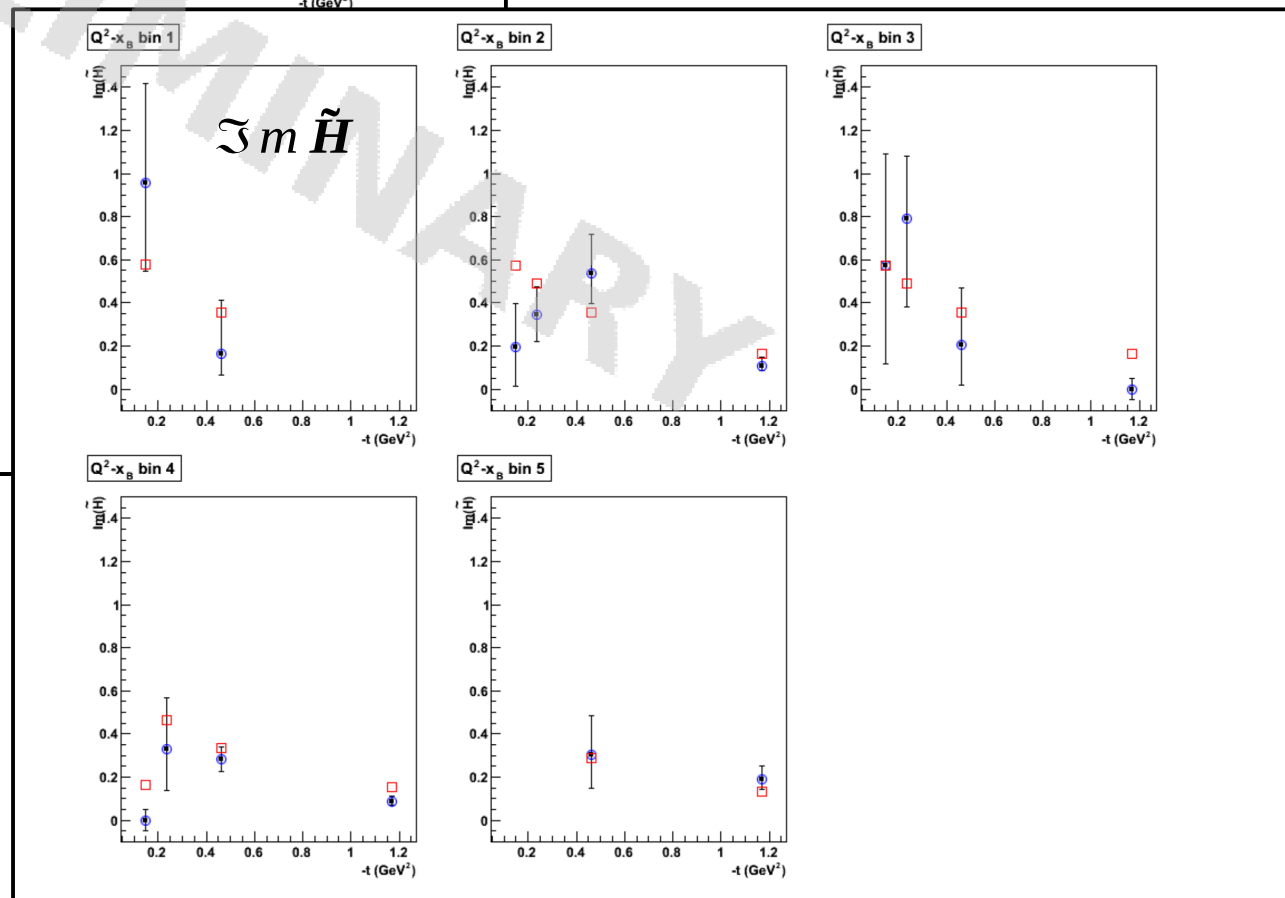

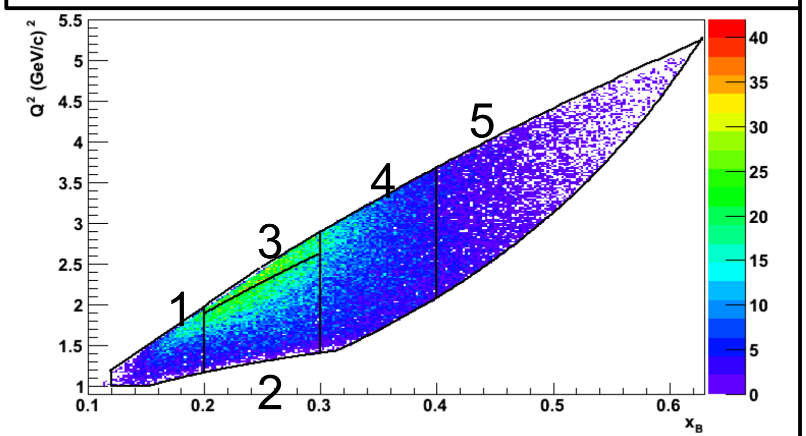

- VGG model predictions
- Extracted values (M. Guidal)

CFF Extraction

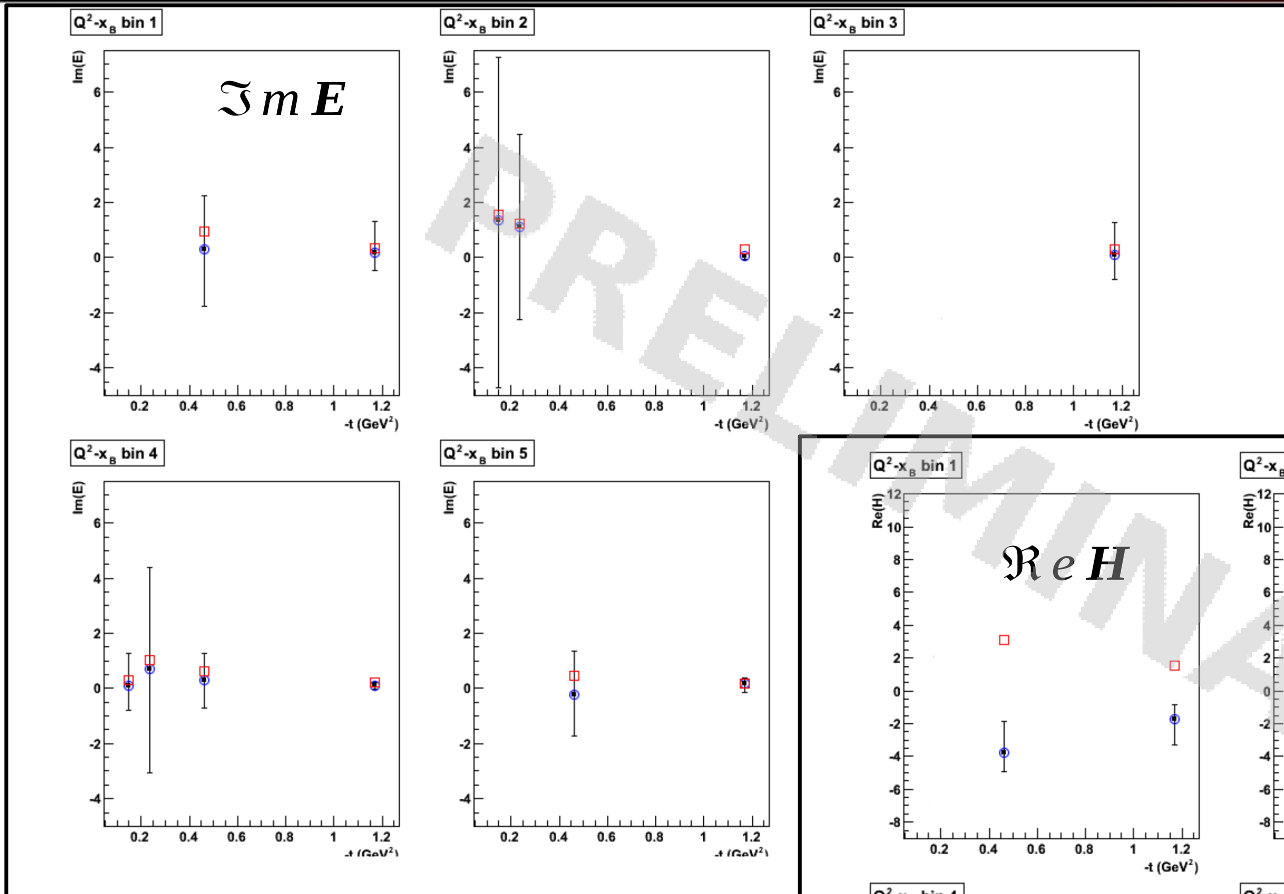

- VGG model predictions
- Extracted values (M. Guidal)

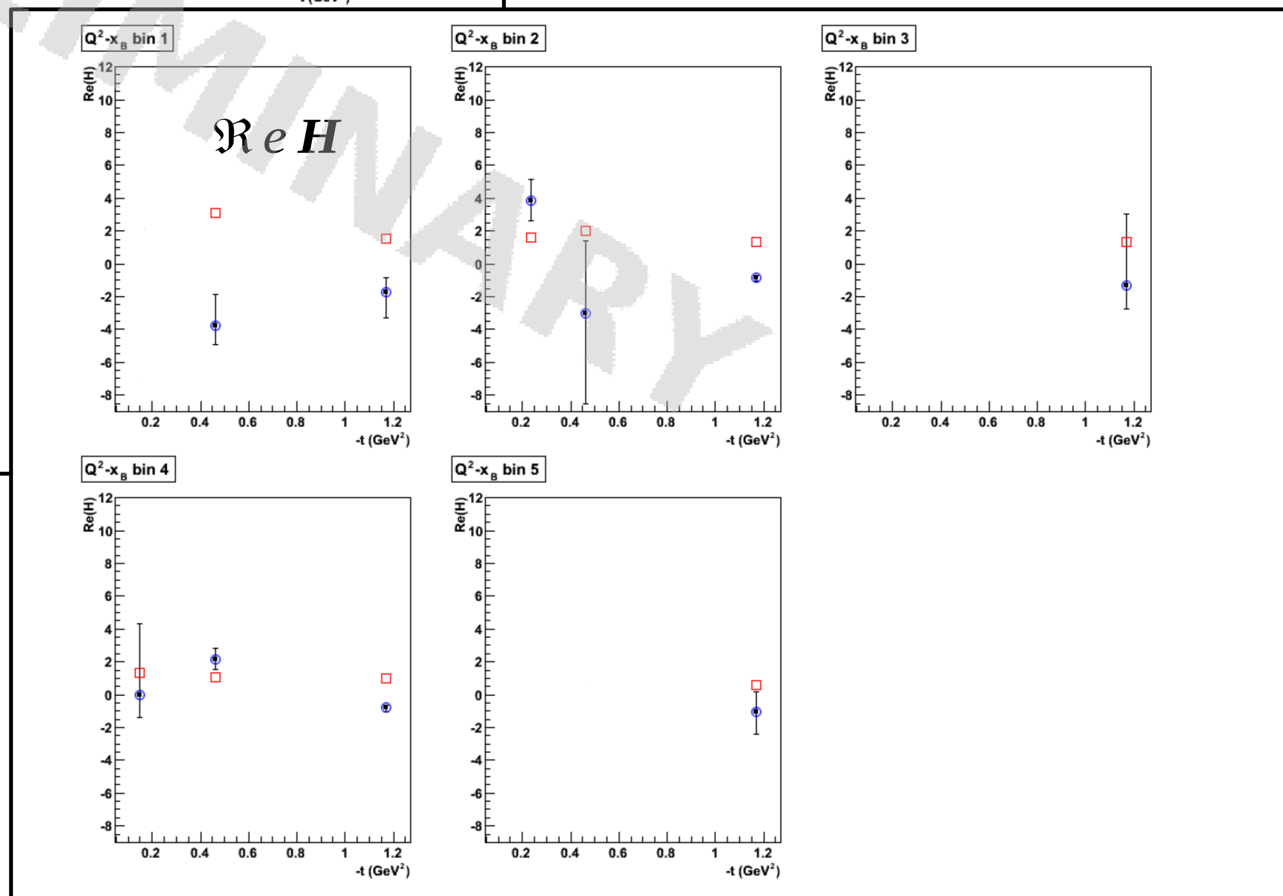

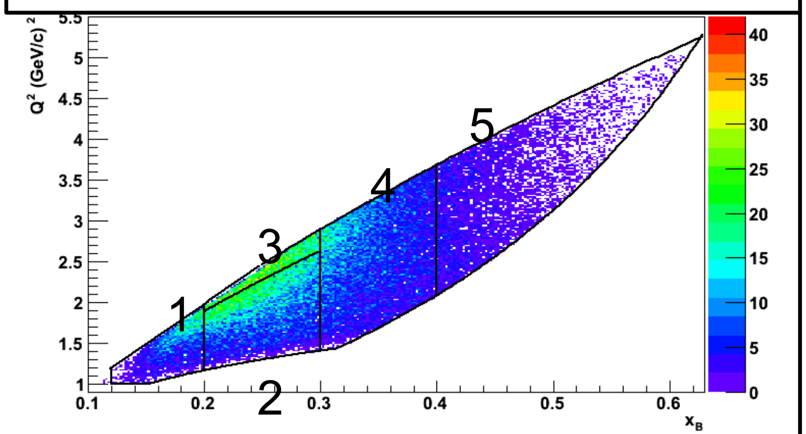

Summary

- GPDs provide a unique tool to study the internal dynamics of the nucleon.
- Their unambiguous extraction from experimental data requires many measurements including DVCS spin observables across large regions of phase space.
- The eg1-dvcs experiment was the first DVCS-dedicated longitudinally polarized target experiment performed with the CLAS detector.
- The simultaneous presence of a polarized beam and longitudinally polarized target allowed extraction of 3 polarization observables: beam-spin, target-spin and double-spin asymmetries, over a wide Q^2, x_B, and t phase space.
- The measurement of the 3 DVCS observables in the same kinematic regions provides more constraints than previously available for GPD extraction.
- The Future: JLab12 GeV and CLAS upgrades will increase the available kinematic regions essential for the continuation of the DVCS program for high precision studies of nucleon structure in the valence region.